iScience

CellPress
OPEN ACCESS

Article

Identification of CX3CR1^{+} mononuclear phagocyte subsets involved in HIV-1 and SIV colorectal transmission

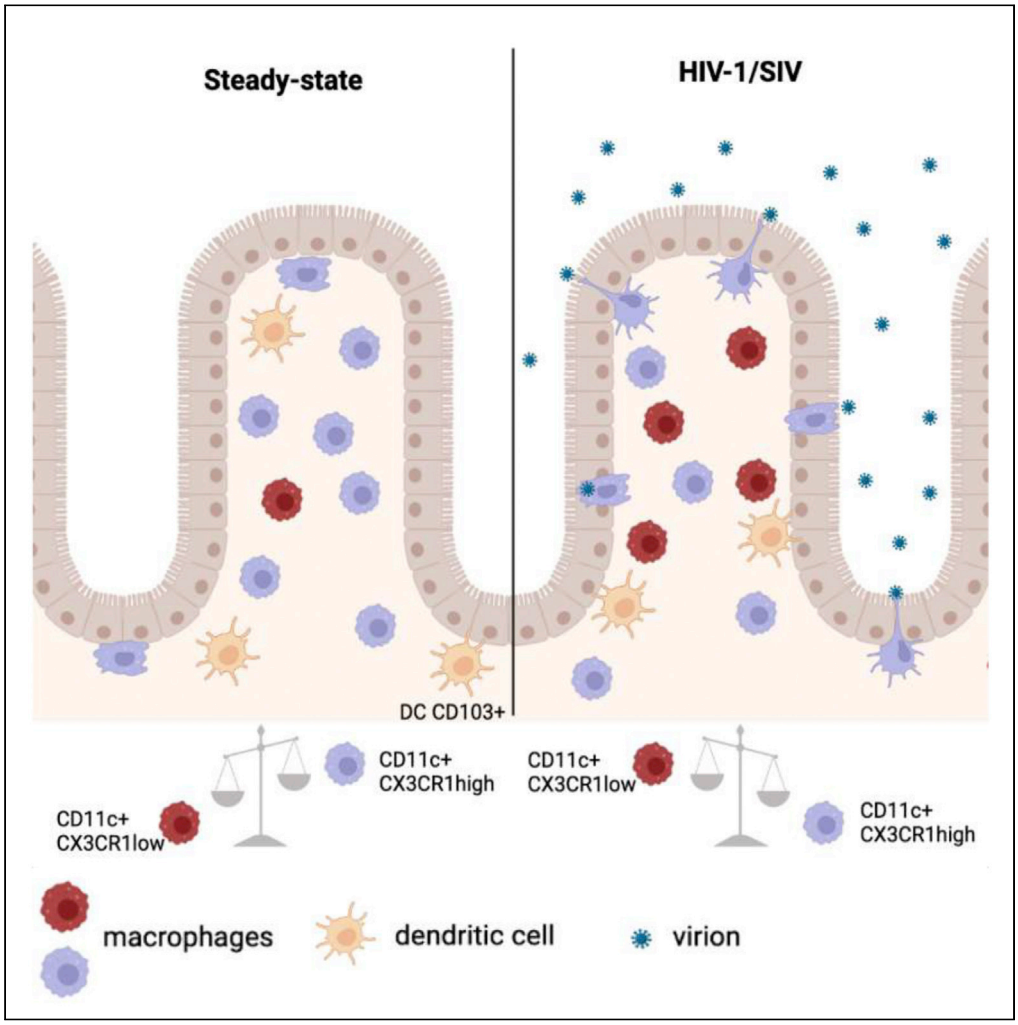

Mariangela Cavarelli, Chiara Foglieni, Naima Hantour, ..., Nathalie Dereuddre-Bosquet, Gabriella Scarlatti, Roger Le Grand

mariangela.cavarelli@cea.fr

Highlights

Human and macaque intestinal MNPs show similar phenotype, localization, and function

CX3CR1^{+} MNPs migrate inside the intestinal epithelium to sample HIV/SIV

SIV infection alters the balance between CX3CR1^{high} and CX3CR1^{low} Mφs

CX3CR1^{+} Mφs contribute to the breakdown of the intestinal barrier in HIV/SIV infection

Cavarelli et al., iScience 25, 104346
June 17, 2022
https://doi.org/10.1016/j.isci.2022.104346

iScience

CellPress
OPEN ACCESS

Article

Identification of CX3CR1$^+$ mononuclear phagocyte subsets involved in HIV-1 and SIV colorectal transmission

Mariangela Cavarelli,[1,8,*] Chiara Foglieni,[2] Naima Hantour,[1] Tilo Schorn,[3,6] Antonello Ferrazzano,[3,7] Stefania Dispinseri,[3] Delphine Desjardins,[1] Ugo Elmore,[4,5] Nathalie Dereuddre-Bosquet,[1] Gabriella Scarlatti,[3] and Roger Le Grand[1]

SUMMARY

The difficulty to unambiguously identify the various subsets of mononuclear phagocytes (MNPs) of the intestinal *lamina propria* has hindered our understanding of the initial events occurring after mucosal exposure to HIV-1.

Here, we compared the composition and function of MNP subsets at steady-state and following *ex vivo* and *in vivo* viral exposure in human and macaque colorectal tissues.

Combined evaluation of CD11c, CD64, CD103, and CX3CR1 expression allowed to differentiate *lamina propria* MNPs subsets common to both species. Among them, CD11c$^+$ CX3CR1$^+$ cells expressing CCR5 migrated inside the epithelium following *ex vivo* and *in vivo* exposure of colonic tissue to HIV-1 or SIV. In addition, the predominant population of CX3CR1^{high} macrophages present at steady-state partially shifted to CX3CR1^{low} macrophages as early as three days following *in vivo* SIV rectal challenge of macaques.

Our analysis identifies CX3CR1$^+$ MNPs as novel players in the early events of HIV-1 and SIV colorectal transmission.

INTRODUCTION

Human immunodeficiency virus type 1 (HIV-1) transmission across the colorectal mucosa is the most common mode of acquisition of the virus in western countries (Baldwin and Baldwin, 2000; Misegades et al., 2001). A better understanding of the early target cells and mechanisms that allow HIV-1 passage across the colorectal mucosa could guide the development of prevention strategies aimed at blocking viral entry and spread.

Research on simian immunodeficiency virus (SIV) in nonhuman primates has provided invaluable insights on the pathogenesis of HIV-1 infection. However, the interpretation of results from pathogenic studies and vaccine trials may be biased by possible differences between simian and human mucosa in terms of the phenotype, frequency, and function of target cells present at the site of viral entry. Consequently, the cross-validation of relevant findings in both species is required.

The mononuclear phagocyte (MNP) population that resides in the lower intestinal tract of humans and macaques includes numerous subsets of dendritic cells (DCs) and macrophages (Mφs), shown to be among the first target cells encountered by the virus (Cavarelli et al., 2013; Cavarelli and Scarlatti, 2014). Indeed, CD11c$^+$ HLA-DR$^+$ DCs from the human jejunal mucosa were shown to rapidly transmit HIV-1 infection (Shen et al., 2010) and those from the human colonic mucosa to sample luminal R5 HIV-1 through an envelope-CCR5-mediated mechanism (Cavarelli et al., 2013) in *ex vivo* tissue models. Consistent with these observations, CD11c$^+$ HLA-DR$^+$ cells of the cynomolgus macaque colonic *lamina propria* similarly respond to SIVmac251 stimulation *ex vivo* (Cavarelli et al., 2021), further demonstrating that rapid recruitment of these target cells inside the intestinal epithelium is involved in the early steps of viral dissemination. Recently, two cell subsets in the human colonic mucosa, CD14$^+$ CD1c$^+$ monocyte-derived DCs and langerin-expressing conventional DC2, were reported to be involved in HIV-1 uptake and transmission *ex vivo* (Rhodes et al., 2021).

Although tissue resident Mφs have been less studied than DCs, human jejunum Mφs have been reported to support HIV-1 replication (Li et al., 1999; Smith et al., 1997a, 1997b) and Mφs from the rectum to

[1]Université Paris-Saclay, Inserm, CEA, Center for Immunology of Viral, Autoimmune, Hematological and Bacterial Diseases (IMVA-HB/IDMIT), 18, route du Panorama 92265 Fontenay-aux-Roses, Le Kremlin-Bicêtre, France

[2]Myocardial Diseases and Atherosclerosis Unit, IRCCS Ospedale San Raffaele, Milan, Italy

[3]Viral Evolution and Transmission Unit, IRCCS Ospedale San Raffaele, Milan, Italy

[4]Department of Gastrointestinal Surgery, IRCCS Ospedale San Raffaele, Milan, Italy

[5]School of Medicine and Surgery, Università Vita-Salute San Raffaele, Milan, Italy

[6]Present address: MetaSystems s.r.l., Milan, Italy

[7]Present address: AGC Biologics S.P.A., Cell Process Development Unit, Milan, Italy

[8]Lead contact

*Correspondence: mariangela.cavarelli@cea.fr

https://doi.org/10.1016/j.isci.2022.104346

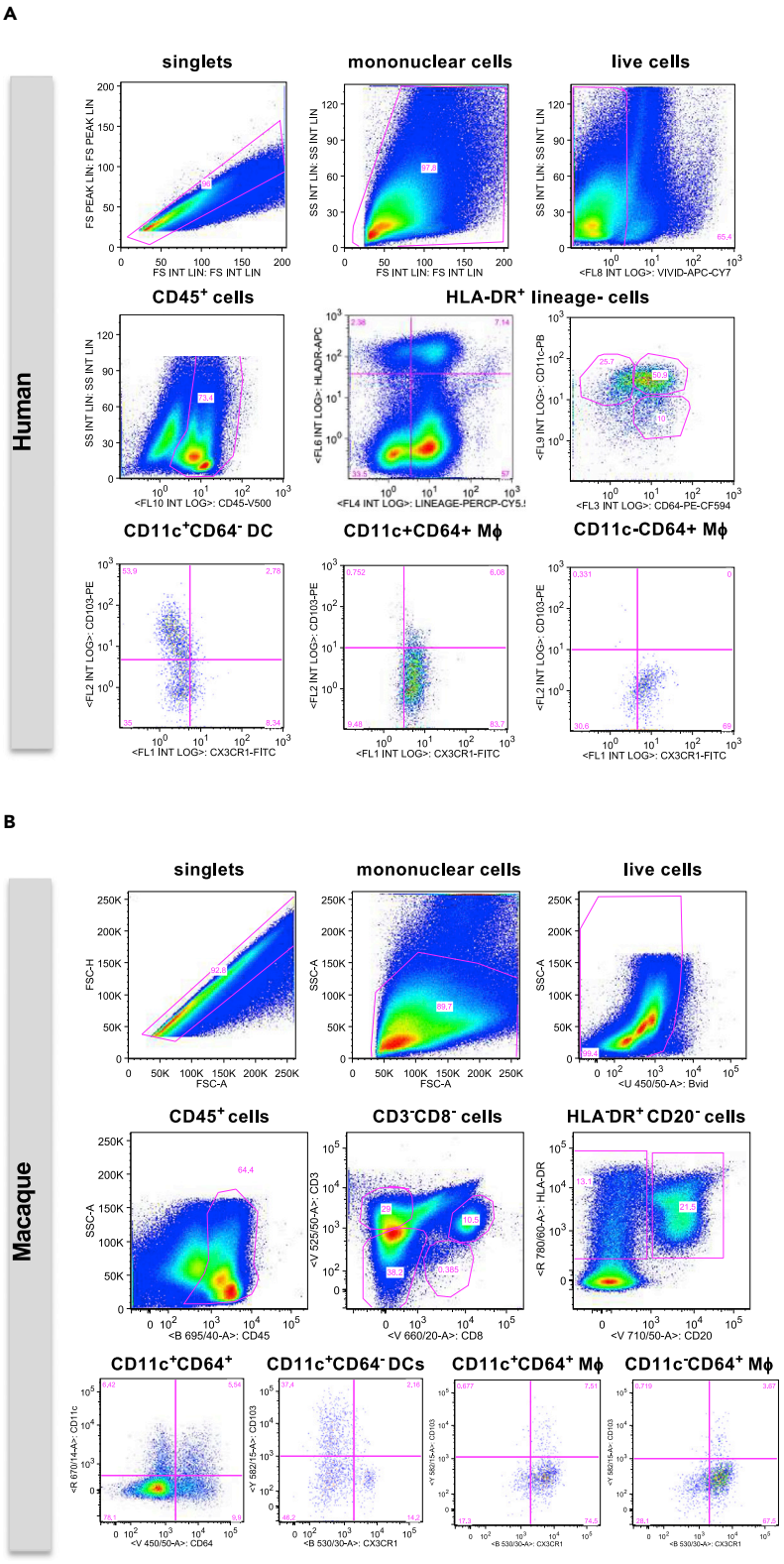
A
Human
singlets
mononuclear cells
live cells
CD45+ cells
HLA-DR+ lineage- cells
CD11c+CD64- DC
CD11c+CD64+ Mϕ
CD11c-CD64+ Mϕ
B
Macaque
singlets
mononuclear cells
live cells
CD45+ cells
CD3-CD8- cells
HLA-DR+CD20- cells
CD11c+CD64+
CD11c+CD64- DCs
CD11c+CD64+ Mϕ
CD11c-CD64+ Mϕ
C
% of CD45+ cells among live cells
Human
Macaque
D
% of Lineage- HLA-DR+ cells among CD45+ cells
**
Human
Macaque
E
Human
**
% of CD45+ cells
CD11c+CD64- DC
CD11c+CD64+ Mϕ
CD11c-CD64+ Mϕ
F
Macaque
**
**
% of CD45+ cells
CD11c+CD64- DC
CD11c+CD64+ Mϕ
CD11c-CD64+ Mϕ

Figure 1. Phenotypic characterization of lamina propria mononuclear phagocytes in the human and macaque colon

(A and B) Representative flow cytometry plots of MNPs in untreated and morphologically preserved human (A) and macaque (B) colon. Leukocytes are identified among live cells as $CD45^+$. Three subsets of MNPs were identified based on the expression of CD11c and CD64 within single, viable, $CD45^+$ $HLA\text{-}DR^+$ $lineage^-$ cells: $CD11c^+$ $CD64^-$ DCs, $CD11c^+$ $CD64^+$ Mφs, and $CD11c^-$ $CD64^+$ Mφs.

(C and D) The frequency of (C) $CD45^+$ cells and (D) $HLA\text{-}DR^+/lineage^-$ cells (E, F) are shown. Symbols: DCs and Mφs in humans = round symbols; macaques = squared symbols; colon sample number: n = 12 for human and n = 10 for macaque tissues. The mean ± the SD is plotted. Mann-Whitney tests were used to compare the frequency of cells between human and macaque colon, whereas Friedman tests with FDR correction were used to compare DC and Mφ numbers within the same colon donor. p-values < 0.05 were considered significant (*$p < 0.05$, **$p < 0.01$, ***$p < 0.001$).

constitutively express CCR5 (McElrath et al., 2013), thus being potential HIV-1 target cells. However, the distinction between Mφs and DCs in the intestinal *lamina propria* based on major surface markers is not always conclusive, and the inability to clearly differentiate between them makes it difficult to define the relative role of each subset in HIV/SIV acquisition and pathology. Indeed, aside from classic Mφs, the gut also contains an atypical population of Mφs that express CD11c, a marker previously specifically associated with DCs (Bradford et al., 2011). Human intestinal $CD11c^+$ Mφs have been recently shown to be immature, loosing CD11c expression with maturation (Bujko et al., 2018). Moreover, DCs can be distinguished from other MNPs, such as monocytes and monocyte-derived Mφs, by their lack of expression of the high-affinity IgG receptor FcγRI, CD64 (Tamoutounour et al., 2012). In contrast to DCs, $CD64^+$ MNPs do not express the integrin αE chain CD103 and include all chemokine CX3C receptor $(CX3CR)1^{high}$ cells, which are tissue-resident Mφs (Bain et al., 2012; Persson et al., 2013; Tamoutounour et al., 2012). The $CD64^+$ population also contains a subset of $CX3CR1^{int/low}$ cells, representing an intermediate stage in the local differentiation of tissue-resident Mφs (Desalegn and Pabst, 2019; Tamoutounour et al., 2012). Of note, intestinal $CX3CR1^{high}$ Mφs have been shown to be abundant in the steady-state and to have an anti-inflammatory phenotype, whereas $CX3CR1^{low}$ Mφs are more abundant in the inflamed intestine and adopt a pro-inflammatory phenotype (Bain et al., 2012; Desalegn and Pabst, 2019). Finally, a discrete population of DCs expressing low levels of CX3CR1 has also been identified in both the mouse and human gut (Bujko et al., 2018; Persson et al., 2013).

Mouse studies have shown that $CD103^+$ and $CX3CR1^+$ cells play different roles in antigen sampling. $CD103^+$ cells are considered to be *bona fide* DCs, able to migrate to mesenteric lymph nodes upon Toll-like receptor (TLR) stimulation (Varol et al., 2009), priming naive T cells (Schulz et al., 2009). Conversely, $CX3CR1^+$ Mφs are able to shuttle across the epithelium to collect bacterial antigens (Niess et al., 2005) but unable to migrate to mesenteric lymph nodes (Schulz et al., 2009). Although abundant in the colorectal mucosa, $CX3CR1^+$ MNPs have been mostly overlooked in studies on HIV-1 transmission. Moreover, the composition and function of the intestinal MNP subset is still a subject of debate (Chiaranunt et al., 2021) and needs to be clarified in the context of mucosal HIV/SIV infection.

Here, we extensively characterized the MNP subsets that reside in the resting colorectal mucosa of both humans and cynomolgus macaques and analyzed their dynamics following *ex vivo* and *in vivo* viral exposure. We found that $CD11c^+$ DCs and Mφs expressing CX3CR1, but not $CD11c^+$ $CD103^+$ DCs, insert themselves in between intestinal epithelial cells to sample luminal virions following *ex vivo* and *in vivo* viral exposure. *In vivo*, we show that the abundance of these cells in the intestinal *lamina propria* decreased as soon as three days post-SIVmac251 exposure. Among them, $CX3CR1^+$ DCs appeared to accumulate in the draining lymph nodes, whereas Mφs remained *in situ* while switching from a tissue-resident $CX3CR1^{high}$ to a pro-inflammatory $CX3CR1^{low}$ phenotype. Our results reveal a novel role for $CX3CR1^+$ MNPs in the early events of HIV/SIV transmission.

RESULTS

Characterization of mononuclear phagocyte subsets of the human and macaque colonic lamina propria

Colonic *lamina propria* MNPs were identified among living $CD45^+$ cells as $HLA\text{-}DR^+$ $lineage^-$ cells (lineage defined as $CD3^-CD56^-CD19^-CD16^-$ for human tissue samples and $CD3^-CD8^-CD20^-$ for macaques) by flow cytometry (Figures 1A and 1B). Among the $CD45^+$ cells, which represented approximately 50% of the recovered living cells from both species (Figure 1C), the frequency of $HLA\text{-}DR^+$ $lineage^-$ cells was 3.6 ± 1.8% in the human and 5.8 ± 2% in the macaque colon tissue (Figure 1D). Analysis of CD11c and CD64 showed three distinct populations in both the human (Figures 1A and 1E) and macaque (Figures 1B and 1F) mucosa: i.e. $CD11c^+$ $CD64^-$ myeloid DCs, $CD11c^+$ $CD64^+$ Mφs, and $CD11c^-$ $CD64^+$ Mφs.

In the human colon, the abundance of CD11c$^+$ CD64$^+$ immature Mφs was significantly higher than that of CD11c$^-$ CD64$^+$ mature Mφs (1.5 ± 0.8% and 0.7 ± 0.6% CD45$^+$ cells, respectively, p = 0.009), whereas we observed mostly mature Mφs in the macaque tissue (0.2 ± 0.1% and 0.7 ± 0.8% CD45$^+$ cells, respectively, p = 0.0018). The frequency of immature Mφs was significantly lower than that of CD11c$^+$ CD64$^-$ DCs in the macaque tissue (p = 0.0019). CD11c$^+$ CD64$^-$ DCs represented 0.9 ± 0.4% of CD45$^+$ cells in the human and 0.34 ± 0.15% in the macaque *lamina propria* (Figures 1E and 1F).

Assessment of CD103 and CX3CR1 expression by CD11c$^+$ CD64$^-$ DCs, CD11c$^+$ CD64$^+$ Mφs, and CD11c$^-$ CD64$^+$ Mφs was performed, and gate was positioned based on the fluorescence minus one (FMO) controls (Figures 1A, 1B and S1).

Comparisons of DC subsets showed CD103$^+$ CX3CR1$^-$ DCs to be similarly distributed in both species (36.9 ± 15.7% of DCs in humans and 32.1 ± 10.2% in macaques, Figure 2A). However, CD103$^-$ CX3CR1$^-$ DCs represented 60.7 ± 14.9% of total DCs in humans and 33.5 ± 18.9% in macaque tissues. CD103$^-$ CX3CR1$^+$ DCs represented a discrete population of cells that was rare in the human colon but more common in that of the macaques (2.1 ± 2.2% versus 19.3 ± 7.7% of DCs). We did not observe cells expressing both CD103 and CX3CR1 in either species. CX3CR1 levels were lower on DCs relative to both CD11c$^+$ and CD11c$^-$ CD64$^+$ Mφs (Figure 2B), as previously described in the mouse lamina propria (Persson et al., 2013).

Further analysis showed varying levels of CX3CR1 for both CD11c$^+$ and CD11c$^-$ colonic Mφs, which allowed us to differentiate, among CD103$^-$ cells, two subsets: CX3CR1^{high} and CX3CR1^{low} (Figures 2C and 2D). In the human colon, we detected 83.7 ± 17.4% CD103$^-$CX3CR1^{high} CD11c$^+$ Mφ and 83.6 ± 13.7% CD103$^-$ CX3CR1^{high} CD11c$^-$ Mφs (Figure 2E). Approximately 15% of both CD11c$^+$ and CD11c$^-$ Mφ were CD103$^-$ CX3CR1^{low} cells. As in human tissues, in macaque the Mφs were mostly CX3CR1^{high}, independently of CD11c expression (94.5 ± 5.9% of CD11c$^+$ Mφs and 85.4 ± 13.1% of CD11c$^-$ Mφs, Figure 2F). In contrast to DCs, CD103 was virtually absent from all colonic Mφs of both species (Figures 2E and 2F).

Overall, these results show that, despite differences between the immature/mature Mφ ratio, the same subsets of DCs and Mφs are present in human and macaque colonic mucosa.

Similar distribution of mononuclear phagocyte subsets at steady state in human and macaque colonic lamina propria by microscopic analysis

We analyzed at confocal microscope the tissue distribution of the various cell subsets identified by flow cytometry, combining CD11c with CD103, CX3CR1, or CD64 labeling (Figure 3).

We observed CD11c$^+$ CD103$^-$ MNPs, CD11c$^-$ CD103$^+$ lymphocytes, and CD11c$^+$ CD103$^+$ DCs in both human (Figures 3A and 3D) and macaque mucosal tissues (Figures 3G and 3J). Among them, cells positive for one marker only were mostly apical, whereas those expressing both markers were localized more deeply inside the *lamina propria*.

CD11c$^+$ CX3CR1$^+$ cells, i.e., Mφs, and, to a lesser extent, DCs, as well as CD11c$^+$ CX3CR1$^-$ and CD11c$^-$ CX3CR1$^+$ cells, were detected. However, the two latter subsets were more frequently found (Figures 3B and 3E shows human cells and Figures 3H and 3K macaque cells).

Finally, both CD11c$^+$ CD64$^+$ immature and CD11c$^-$ CD64$^+$ mature Mφs and CD11c$^+$ CD64$^-$ DCs were detected throughout the mucosa (Figures 3C and 3F shows human cells and Figures 3I and 3L macaque cells). In line to what previously described (Han et al., 2021; Sagaert et al., 2012), Mφs were often detected in the sub-epithelial region of the intestinal mucosa.

The HIV-1 coreceptor CCR5 is preferentially expressed by CD11c$^+$ CX3CR1$^+$ mononuclear phagocytes rather than by CD11c$^+$ CD103$^+$ DCs

We showed that the interaction between the HIV-1 envelope and CCR5 coreceptor induced the migration of *lamina propria* CD11c$^+$ cells to the epithelium to capture luminal virions (Cavarelli et al., 2013). Therefore, we analyzed CCR5 expression by colonic DC and Mφ subsets in tissues from five macaques by flow cytometry. Both CD11c$^+$ and CD11c$^-$ Mφs showed higher CCR5 expression than DCs (p = 0.0039 and 0.0085, respectively, Kruskal-Wallis test with FDR correction), with CD64$^-$ DCs being predominantly CCR5$^-$ cells

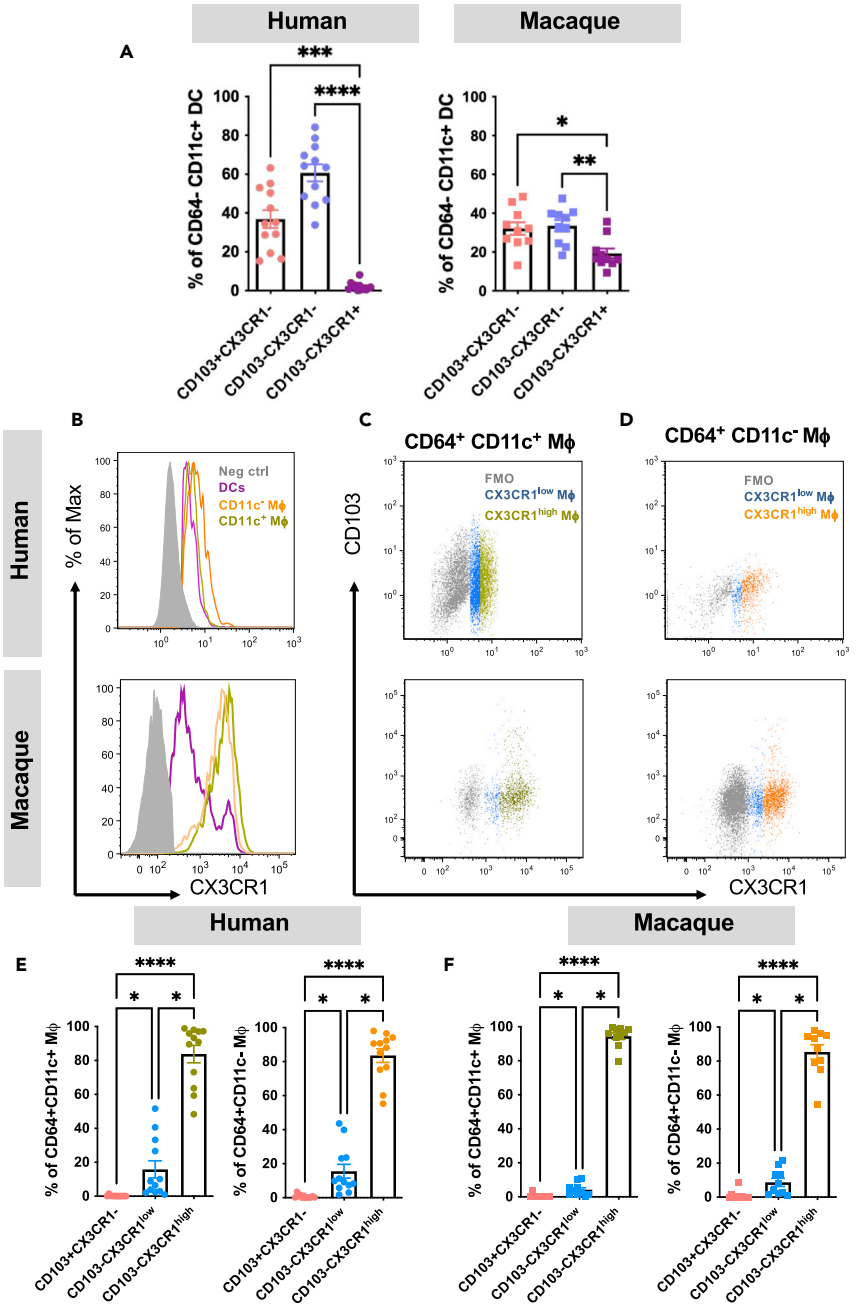

Figure 2. Definition of DC and Mφ subsets

(A) Relative proportion of CD103$^+$ CX3CR1$^-$, CD103$^-$ CX3CR1$^-$, and CX3CR1$^+$ CD103$^-$ CD11c$^+$ CD64$^-$ DCs in human and macaque colonic mucosa.

(B) Human (upper panel) and macaque (lower panel) CD11c$^+$ CD64$^-$ CX3CR1$^+$ DCs expressing less CX3CR1 relative to CD11c$^+$ CD64$^+$ Mφs and CD11c$^-$ CD64$^+$ Mφs are shown. The shaded histogram is the isotype control.

(C and D) Human (upper panel) and macaque (lower panel) CD11c$^+$ CD64$^+$ Mφs (C) and CD11c$^-$ CD64$^+$ Mφs (D) were divided into CX3CR1^{high} and CX3CR1^{low} subsets relative to the fluorescence minus one (FMO) control (gray).

(E and F) The relative proportion of CD103$^+$ CX3CR1$^-$, CD103$^-$ CX3CR1^{low}, and CD103$^-$ CX3CR1^{high} cells among the CD11c$^+$ CD64$^+$ Mφs and CD11c$^-$ CD64$^+$ Mφs in human (E) and macaque (F) colonic mucosa is displayed. Results were obtained from tissues from12 human donors and 10 macaques. The mean ± the SD is plotted. Friedman tests with FDR correction were applied to the data (*$p < 0.05$, **$p < 0.01$, ***$p < 0.001$, ****$p < 0.001$).

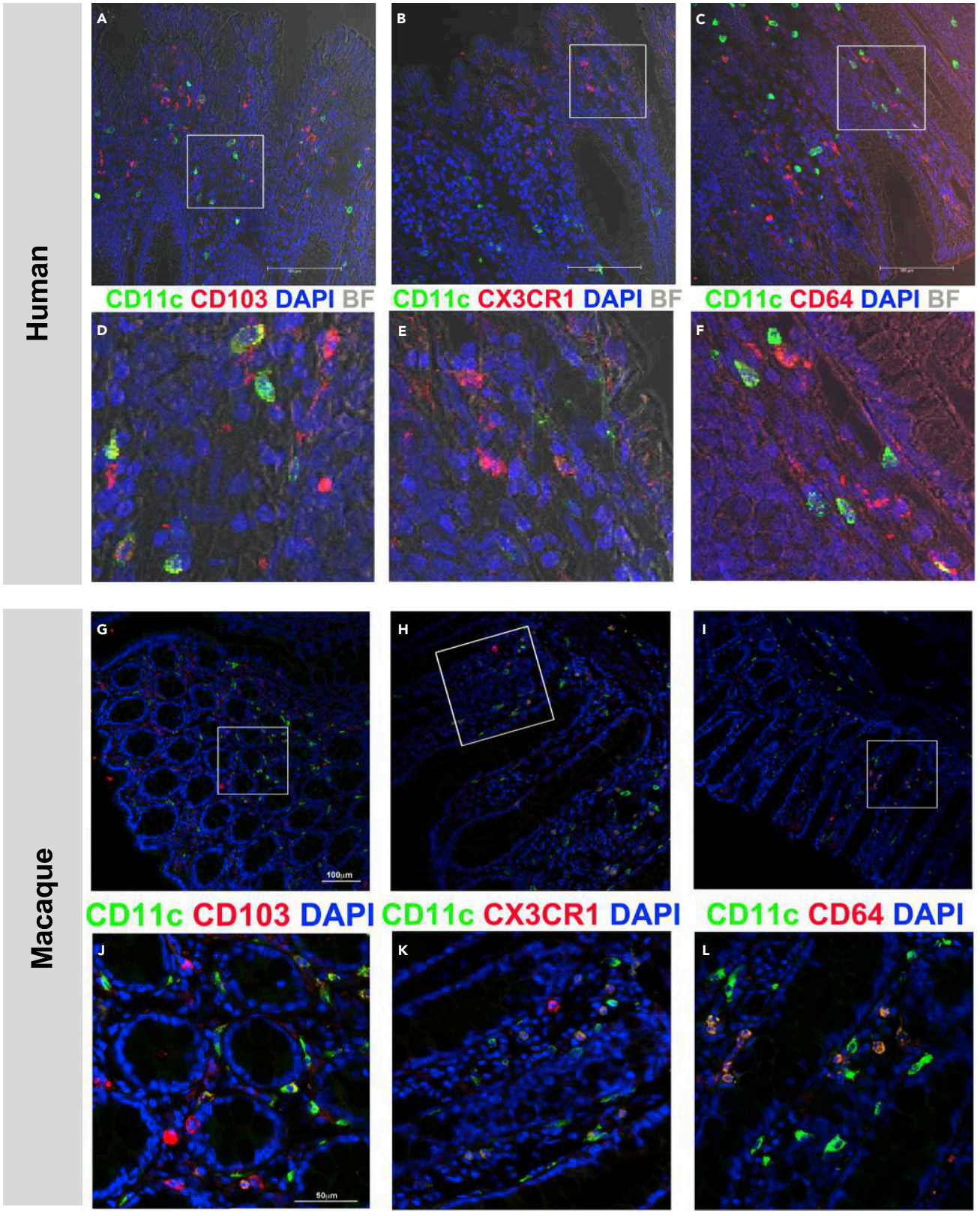
Human
A
B
C
CD11c CD103 DAPI BF
CD11c CX3CR1 DAPI BF
CD11c CD64 DAPI BF
D
E
F
Macaque
G
H
I
100μm
CD11c CD103 DAPI
CD11c CX3CR1 DAPI
CD11c CD64 DAPI
J
K
L
50μm

Figure 3. Distribution of mononuclear phagocyte subsets in human and macaque colonic mucosa at steady state

(A–L) Sections from untreated human (A–F) and macaque (G–L) colonic tissues fixed with 4% PFA and cryopreserved are shown. DC and Mφ subsets were identified by labeling with CD11c-FITC (green) in combination with either CX3CR1-PE, CD103, or CD64, followed by goat-*anti*-mouse Alexa Fluor 594 (red). DAPI (blue) was used to stain the nuclei. The bright field image (BF, gray) was superimposed with the fluorescence images to visualize the contour of the intestinal barrier. The lower panels (D–F and J–L) are magnifications of the boxed area in the upper panel. Scale bars indicate the magnification.

(Figure 4A). This analysis was limited to macaques due to the relatively more abundant colonic tissue available for cell isolation.

The analysis of the HIV-1 co-receptors CCR5 and CXCR4 in tissues from six donors of both species showed that 49.7 ± 14.7% of human and 40.9 ± 20.7% of macaque HLA-DR$^+$ lineage$^-$CD11c$^+$ cells expressed both co-receptors (Figure 4B and gating strategy shown in Figure S2). Single-positive CCR5$^+$ cells were more abundant in human (18.3 ± 9.6%) than macaque (2.9 ± 2.04%) colon, whereas proportion of CCR5$^+$ CXCR4$^+$ cells were similar in both species. CCR5 was less expressed by CD11c$^+$ CD103$^+$ (Figure 4C) than CD11c$^+$ CX3CR1$^+$ cells (Figure 4D), consistent with the predominant expression of CCR5 by Mφs relative to DCs observed for macaque cells.

These observations suggest that the CCR5$^+$ CD11c$^+$ CX3CR1$^+$ populations of DCs and Mφs may be more prone to respond to viral stimulation by actively migrating across the epithelium and sampling virions.

CD11c$^+$ CX3CR1$^+$ mononuclear phagocytes, but not CD11c$^+$ CD103$^+$ DCs, migrate to inside the colonic epithelium following exposure to HIV-1 and SIV

We investigated whether exposure of the colorectal mucosa to CCR5 tropic-virus induces differential recruitment of MNP subsets toward the luminal epithelium using the established *ex vivo* polarized explant culture system that mimics the biology of HIV/SIV sexual transmission and the natural route of viral entry into the mucosa (Cavarelli et al., 2013, 2021). Confocal microscopy of human and macaque colonic tissues exposed to cell-free HIV-1 AD8 (Figures 5A–5C) or SIVmac251 (Figures 5D–5F), respectively, showed both viruses to induce a comparable migration pattern of DCs and Mφs. Indeed, CD11c$^+$ CD64$^+$ Mφs (Figures 5A and 5D) and CD11c$^+$ CD64$^-$ DCs (Figures 5B and 5E) were detected in between cells of the intestinal epithelium following 30 min of viral exposure relative to control tissue (Figures 5G and 5J), consistent with the timing of our previous study (Cavarelli et al., 2013). We did not observe intraepithelial migration of CD11c$^-$ CD64$^+$ Mφs. Further characterization showed that migrating cells were CD11c$^+$ CX3CR1$^+$ Mφs and CD11c$^+$ CX3CR1$^+$ DCs (Figures 5C and 5F). CX3CR1$^+$ cells in control tissues are shown in Figures 5H and 5K for comparison.

Of note, CD103$^+$ cells physiologically present beneath/within the epithelium were mainly CD3$^+$ lymphocytes and not DCs, as they lacked the expression of CD11c (Figures 5I, 5L, 6A, and 6D). Following viral exposure, intraepithelial CD3$^+$ CD103$^+$ lymphocytes were still detected (Figures 6B and 6C), whereas CD11c$^+$ CD103$^+$ DC recruitment was not induced, neither by HIV-1 (Figures 6B and 6E) nor by SIV (Figures 6C and 6F). Intraepithelial CD11c$^+$ CD103$^-$ MNPs were detected as well (Figure S3).

In summary, HIV-1 and SIV induced intraepithelial recruitment of both CD11c$^+$ Mφs and DCs co-expressing the CX3CR1 receptor, which might act as an initial target of the virus. Neither virus induced recruitment of tolerogenic CD11c$^+$ CD103$^+$ DCs. We also confirmed previous observations that CD3$^+$ lymphocytes are strategically localized to favor viral transmission to the *lamina propria* (McElrath et al., 2013).

In vivo challenge with SIVmac251 induces a rapid shift from CX3CR1^{high} to CX3CR1^{low} phagocytes in the macaque colonic mucosa

We investigated whether the identified MNP subsets populating the colonic *lamina propria* are differentially affected in the early phases of SIV infection by performing an *in vivo* study. Three cynomolgus macaques were intrarectally exposed to SIVmac251 and euthanized 72h later. MNP subset migration patterns and relative cell frequency were assessed by confocal microscopy and flow cytometry, respectively, and compared with those of ten untreated animals (those characterized earlier).

Analogous to what we observed in *ex vivo*-treated tissues, we detected the presence of intraepithelial MNPs, specifically CD11c$^+$ CD64$^+$ and CD11c$^+$ CX3CR1$^+$ cells (Figures 7A–7C). Intraepithelial CD11c$^+$ CD103$^+$ cells were not observed. However, in contrast to our *ex vivo* observations after 30 min of viral

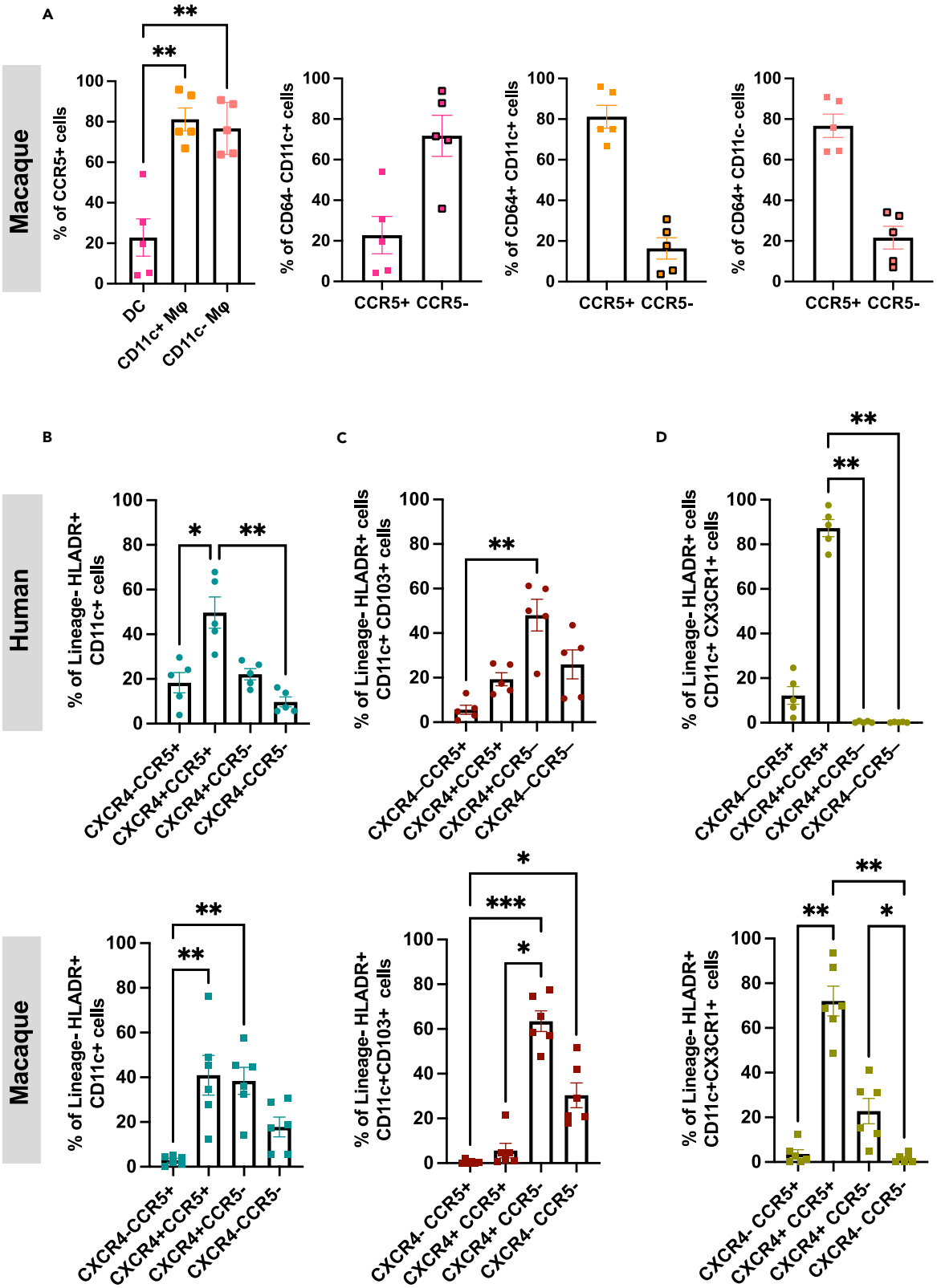
A
Macaque
% of CCR5+ cells
DC
CD11c+ Mφ
CD11c- Mφ
% of CD64- CD11c+ cells
% of CD64+ CD11c+ cells
% of CD64+ CD11c- cells
CCR5+ CCR5-
B
C
D
Human
% of Lineage- HLADR+ CD11c+ cells
% of Lineage- HLADR+ cells CD11c+ CD103+ cells
% of Lineage- HLADR+ cells CD11c+ CX3CR1+ cells
CXCR4-CCR5+
CXCR4+CCR5+
CXCR4+CCR5-
CXCR4-CCR5-
Macaque
% of Lineage- HLADR+ CD11c+ cells
% of Lineage- HLADR+ CD11c+CD103+ cells
% of Lineage- HLADR+ CD11c+CX3CR1+ cells
CXCR4- CCR5+
CXCR4+ CCR5+
CXCR4+ CCR5-
CXCR4- CCR5-

Figure 4. HIV-1 coreceptor expression by mononuclear phagocytes

Immune phenotyping was performed as described in STAR Methods and Table S1.

(A–D) Proportion of CD11c$^+$ CD64$^-$ DCs, CD11c$^+$ CD64$^+$ Mφs, and CD11c$^-$ CD64$^+$ Mφs expressing the CCR5 receptor in the colonic mucosa from five macaques CCR5 and CXCR4 expression by (B) total CD11c$^+$ HLA-DR$^+$ lineage- MNPs, (C) CD11c$^+$ CD103$^+$ MNPs, and (D) CD11c$^+$ CX3CR1$^+$ MNPs in human (n = 5) and macaque (n = 6) colon samples is presented. The mean ± the SD is plotted. Wilcoxon rank pairs tests were applied in panel A, whereas Friedman tests with FDR correction were used in panels B–D. p-values < 0.05 were considered significant (*p < 0.05, **p < 0.01, ***p < 0.001).

exposure, *in vivo*, after 72h of viral exposure, the intraepithelial cells were mostly found in the crypts and rarely inside the luminal epithelium.

As expected, we did not observe overt signs of systemic infection at such an early time point. Virus remained undetectable in blood of all except one animal, which had 227 copies/mL. The number of colonic *lamina propria* CD4$^+$ and CD8$^+$ lymphocytes in SIV-exposed macaques was comparable to controls (Figures S4A and S4B), whereas, CD11c$^-$ CD123$^+$ plasmacytoid DCs were significantly depleted (0.07 ± 0.05 versus 0.007 ± 0.003%, p = 0.0280, Mann-Whitney test, Figure S4C).

The total number of *lamina propria* DCs and Mφs (both CD11c$^+$ and CD11c$^-$ subsets) did not change following viral exposure (Figure 7D), but the relative proportions of the various MNP subsets did. Specifically, there was a significant lower proportion of CX3CR1^{high} CD11c$^+$ and CD11c$^-$ Mφs in SIV-exposed animals compared with controls (94.5 ± 5.9% versus 57.4 ± 4.5% p = 0.007 and 85.4 ± 13.1 versus 50.4 ± 6.8% p = 0.0140, respectively) (Figures 7E, 7F, and S5). These changes were paralleled by a statistically significant higher proportion of CX3CR1^{low} cells in both subsets in exposed versus unexposed animals (4.2 ± 3.7 vs 36.4 ± 2.8% p = 0.007 for the CD11c$^+$ subset and 8.7 ± 7.4 vs. 34.5 ± 4.8% for the CD11c$^-$ subset, p = 0.007) (Figures 7E and 7F), suggesting an accumulation of pro-inflammatory Mφs. We also observed a decrease in the proportion of CX3CR1$^+$ DCs (p = 00,088), whereas that of both CD103$^+$ and CD103$^-$ DC subsets did not change (Figures 7G and S5). No changes in the total number of DCs or Mφs or in the relative proportion of cell subsets were observed in the draining colon lymph nodes (Figure S6). However, lymph nodes from SIV-exposed macaques showed a higher, although not statistically significant, proportion of CX3CR1$^+$ DCs (0.9 ± 0.5% vs 1.5 ± 0.9%, Figure S6D), suggesting possible specific recruitment of these cells from the intestinal mucosa.

We found 15.4 ± 7.6% of CD11c$^-$ and 6.6 ± 3.9% of CD11c$^+$ colonic macaque Mφs being CD14$^+$ CD16$^-$ cells in the steady-state condition (Figure S7) and thus, likely unresponsive to LPS/bacteria stimulation, as previously described in the human intestine (Caër and Wick, 2020; P. Smith et al., 1997a, 1997b; Smythies et al., 2005). Of note, we observed a significant increase in the proportion of CD14$^+$ cells among CD11c$^+$ CX3CR1^{low} Mφs in SIV-exposed animals (7.61 ± 3.9 at 3 dpi versus 5.7 ± 15%, p = 0.0350, Mann-Whitney test, Figure 7H), substantiating the hypothesis of a proinflammatory phenotype of the CX3CR1^{low} cells. No significant changes were, however, observed in the CD11c$^-$ CX3CR1^{low} subset (Figure 7I), although cells from one of three animals showed a strong increase in CD14 expression.

Overall, our results indicate that the CX3CR1$^+$ MNP populations of the colonic mucosa were rapidly and profoundly affected by *in vivo* exposure to SIV, before evident changes of the CD103$^+$ cells.

DISCUSSION

Here, we investigated the role that colorectal *lamina propria* MNP populations play in HIV-1 and SIV transmission. We began by thoroughly identifying and comparing the MNPs present in the colorectal mucosa of humans and cynomolgus macaques, determining five main MNP subsets in both species: three populations of CD64$^-$ DCs (tolerogenic CD103$^+$, nontolerogenic CD103$^-$, and CX3CR1$^+$ DC) and two of CD64$^+$ Mφs (immature CD11c$^+$ and mature CD11c$^-$, both expressing different levels of CX3CR1). The distinction between DC and Mφ phenotypes is challenging due to a proportion of intestinal Mφs expressing CD11c and high levels of MHC class II, markers classically used to identify DCs (Cerovic et al., 2014; Joeris et al., 2017). Moreover, the differentiation between intestinal DCs and Mφs exclusively based on the expression of CD103 and CX3CR1 has been proven to be incorrect, as not all intestinal DCs express CD103 and some also express CX3CR1 (Bujko et al., 2018; Persson et al., 2013). We found that CX3CR1 is expressed at higher levels on Mφs than DCs and that CD64 is specifically expressed by Mφs. These results confirm previously reported human data (Bernardo et al., 2016; Bujko et al., 2018; Persson et al., 2013) and

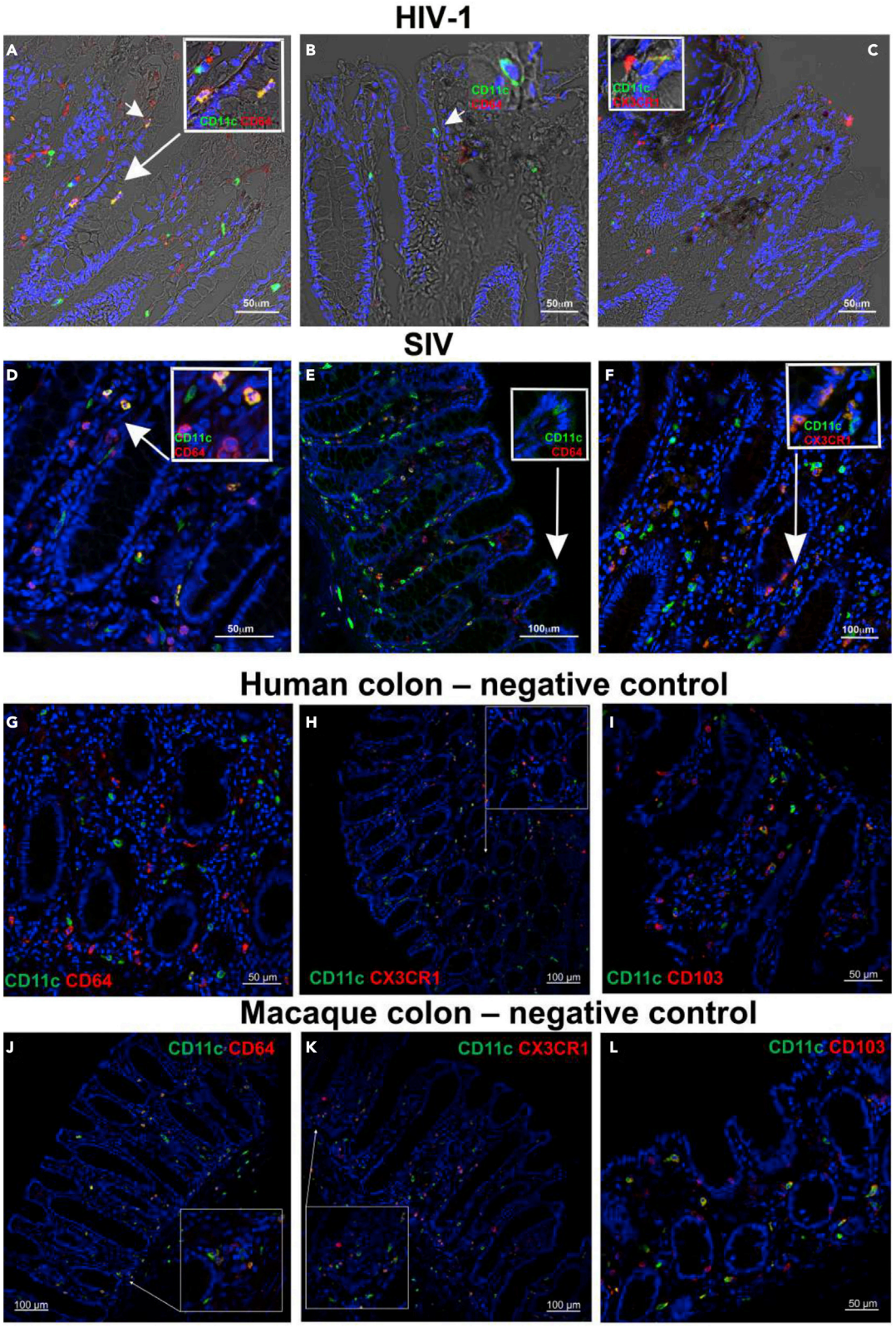
HIV-1
A
CD11c CD64
50μm
B
CD11c
CD64
50μm
C
CD11c
CX3CR1
50μm
SIV
D
CD11c
CD64
50μm
E
CD11c
CD64
100μm
F
CD11c
CX3CR1
100μm
Human colon – negative control
G
CD11c CD64
50 μm
H
CD11c CX3CR1
100 μm
I
CD11c CD103
50 μm
Macaque colon – negative control
J
CD11c CD64
100 μm
K
CD11c CX3CR1
100 μm
L
CD11c CD103
50 μm

Figure 5. Pattern of intraepithelial mononuclear phagocyte recruitment following viral exposure of the colonic mucosa

(A–L) Human (A–C, G–I) and macaque (D–F, J–L) colonic tissues incubated for 30 min either in medium with HIV-1 AD8 (A–C, with brightfield image superimposed to the fluorescence) or SIVmac251 (D–F), or medium only (G–L), fixed with 4% PFA and cryopreserved are shown. Labeling of CD11c-FITC (green) in combination with either CD64 (A, B, D, E) followed by goat-*anti*-mouse Alexa Fluor 594 (red) or CX3CR1-PE (C, F) was performed. Arrows point to subsets of $CD11c^+$ $CD64^+$ (A and D), $CD11c^+$ $CD64^-$ (B and E), and $CD11c^+$ $CX3CR1^+$ (C and F) cells that migrate from the *lamina propria* to in between the epithelial cells following viral exposure. A magnification of the intraepithelial cells is shown in panels A–F (the yellow signal identifies double-positive cells). Magnification of selected regions (indicated by arrows) is shown in the boxed areas of H, J, and K panels. DAPI was used to stain the nuclei. Scale bars indicate the magnification.

extend these observations to nonhuman primates, in which such a detailed characterization of MNP subsets is novel.

Our study led to an alignment of the analytical strategy for human and macaque intestinal MNP characterization, highlighting both similarities and differences between species. We thus found that CD64, CD103, and CX3CR1 expression are a shared feature of intestinal MNPs, whereas immature $CD11c^+$ Mφs were relatively more abundant than mature Mφs in the human mucosa but rare in the macaque mucosa, which is mostly populated by mature $CD11c^-$ Mφs. $CD11c^+$ monocytes have been reported to be recruited to the intestine to undergo conditioning by the microenvironment, leading to an anti-inflammatory and anergic state and differentiation toward $CD11c^-$ Mφs (Bujko et al., 2018). The observed interspecies difference may thus reflect different turnover of intestinal Mφs from blood monocytes.

A major finding of our study was the fundamental difference between the $CX3CR1^+$ and $CD103^+$ subsets in their ability to respond to *ex vivo* viral exposure. Our data show that $CD11c^+$ $CX3CR1^+$ cells, including $CD64^-$ $CD11c^+$ DCs and $CD64^+$ $CD11c^+$ Mφs, are those devoted to extend *trans*-epithelial dendrites or migrate across the tight intestinal epithelium in response to viral stimulation. Thus, here we confirm our previous results but further refine the phenotypic characteristics of these $CD11c^+$ MNPs capable of capturing luminal virions and transfer them to $CD4^+$ T lymphocytes (Cavarelli et al., 2013). The extension of protrusions by migrating cells involved the interaction between their CCR5 receptor and the viral gp120 envelope protein (Cavarelli et al., 2013). Here, we show that both human and macaque $CD11c^+$ $CX3CR1^+$ MNPs expressed higher levels of CCR5 than $CD11c^+$ $CD103^+$ cells, consistent with the observation that the latter ones did not migrate into the epithelium after viral stimulation. The $CD11c^+$ $CX3CR1^+$ MNPs included both DCs and Mφs. Further analysis, including CD64 detection, indicated that macaque $CD64^+$ Mφs showed higher CCR5 levels than $CD64^-$ DCs. Whether the predominance of $CX3CR1^+$ Mφs over $CX3CR1^+$ DC and the higher CCR5 expression might favor Mφs recruitment to the epithelium is puzzling. Nevertheless, $CX3CR1^+$ DC were detected at intraepithelial level *ex vivo* in both species, and the same migration pattern was observed in macaques exposed to SIV *in vivo*.

Given their long lifespan, intestinal Mφs play a key role in HIV-1 persistence. Indeed, although less susceptible to HIV-1 and SIV infection than vaginal Mφs or memory CD4 T cells, intestinal Mφs facilitate HIV-1 entry and carry viral DNA (Moore et al., 2012; Shen et al., 2009), even in HAART-treated patients (Zalar et al., 2010), are resistant to the cytopathic effects of HIV-1 infection/replication, and are able to disseminate the virus (Coleman and Wu, 2009; Ho et al., 1986; Kumar et al., 2014). It is tempting to speculate that the $CD11c^+$ $CX3CR1^+$ Mφs that capture the luminal virions act as viral reservoirs, as recently demonstrated in urethral macrophages (Ganor et al., 2019).

During homeostasis, circulating $CD14^+$ monocytes enter the mucosa to replenish Mφ populations and differentiate into functionally plastic $CD11c^+$ immature cells that rapidly respond to pathogens through phagocytosis and cytokine secretion without inducing inflammation (Bain and Mowat, 2011; Caër and Wick, 2020). It is feasible that HIV-1/SIV not only hijack this response by using $CD11c^+$ cells as carriers but also exploit the sub-epithelial position of $CD11c^+$ $CX3CR1^+$ MNPs to gain access to the intestinal *lamina propria*. Our observation that such a mechanism is favored by $CD11c^+$ $CX3CR1^+$ MNPs but not $CD11c^+$ $CD103^+$ DCs has profound implications on the successive events that lead to dissemination of the virus. It has been reported that $CX3CR1^+$ Mφs do not migrate to draining lymph nodes, whereas they may transfer antigens to migrating DCs in humans and in animal models (Bain and Mowat, 2011; Myoungsoo et al., 2018). Consistent with these data, we did not observe a reduction in the total number of colonic Mφs or $CX3CR1^+$ Mφs accumulation in the draining lymph nodes, which suggest that Mφs remained in the *lamina propria*. In contrast to the behavior of $CX3CR1^+$ Mφs, the number of $CX3CR1^+$ DCs appeared to significantly decrease in the *lamina propria* and showed a tendency to accumulation in the draining lymph nodes, where they likely facilitate infection of $CD4^+$ T cell.

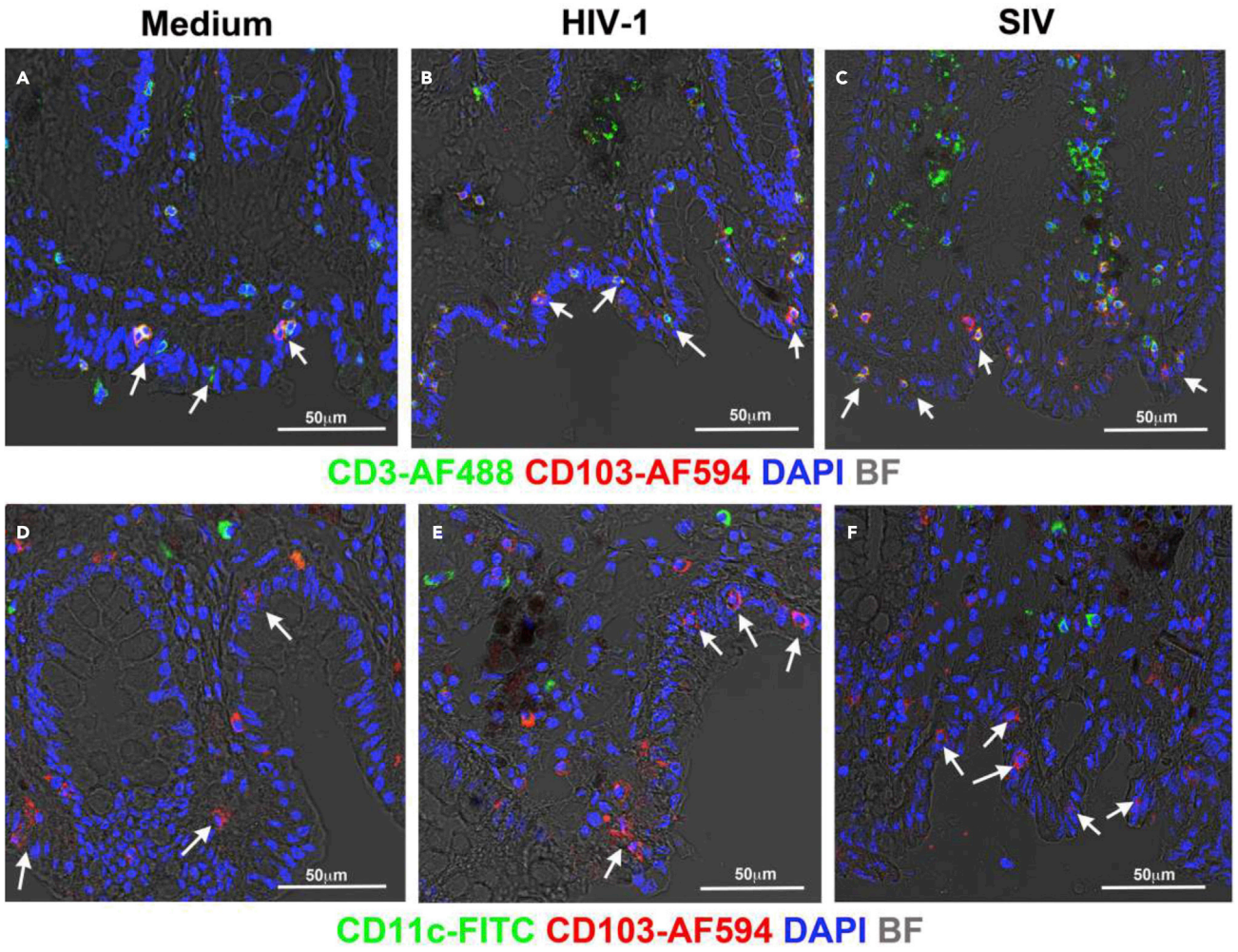

Figure 6. Intraepithelial CD103$^+$ cells are CD3$^+$ T lymphocytes and not CD11c$^+$ DCs

(A–F) Distribution of CD3$^+$ CD103$^+$ T lymphocytes (yellow cells in the upper panels) and CD11c$^+$ CD103$^+$ DCs (yellow cells in the lower panels) and following 30 min of incubation with medium, HIV-1 AD8, or SIV, respectively, are shown. DAPI was used to stain the nuclei (blue). Brightfield images (BF) were superimposed to visualize the intestinal barrier contour. Arrows indicate the intraepithelial cells (or cells partially interposed to epithelium), i.e. CD3$^+$ CD103$^+$ (A–C), CD3$^+$ CD103$^-$ (D–F) and CD11c$^-$ CD103$^+$ (D–F). Scale bars indicate the magnification.

Our findings suggest that the involvement of CX3CR1$^+$ Mφs in HIV pathogenesis goes beyond their ability to extend protrusions. Indeed, we identified two populations of Mφs that express CX3CR1 at different levels, both involved in the early events of HIV-1/SIV transmission. The CX3CR1^{high} versus CX3CR1^{low} subsets have never been investigated in the macaque intestine, although they have been described in the mouse (Bain et al., 2012; Desalegn and Pabst, 2019; Kayama et al., 2012) and, to a lesser extent, in the human intestine (Bernardo et al., 2018). In addition, no other studies examined their role in HIV-1 or SIV transmission. In accordance with the literature, we show that the CX3CR1^{high} subset, known to play an anti-inflammatory role during intestinal homeostasis (Bain et al., 2012; Desalegn and Pabst, 2019; Mowat and Agace, 2014; Weber et al., 2011), predominates in the mucosa at steady-state. Of note, we observed a high prevalence of CX3CR1^{low} Mφs in SIV-exposed macaques *in vivo*. This observation is consistent with the rapid and abundant accumulation of inflammatory CD14$^+$ CD11c$^+$ monocytes differentiating into Mφs, but expressing low levels of CX3CR1, which occurs during intestinal inflammatory events (Bain et al., 2014; Grainger et al., 2017; Weber et al., 2011; Zigmond et al., 2014). Such CX3CR1^{low} Mφs were shown to be highly responsive to stimulation by microbial antigens, subsequently producing pro-inflammatory cytokines (see Li et al., 2021 for a recent review). It has been proposed that the gut microenvironment is unable to commit infiltrating monocytes and differentiating Mφs toward an anti-inflammatory phenotype under

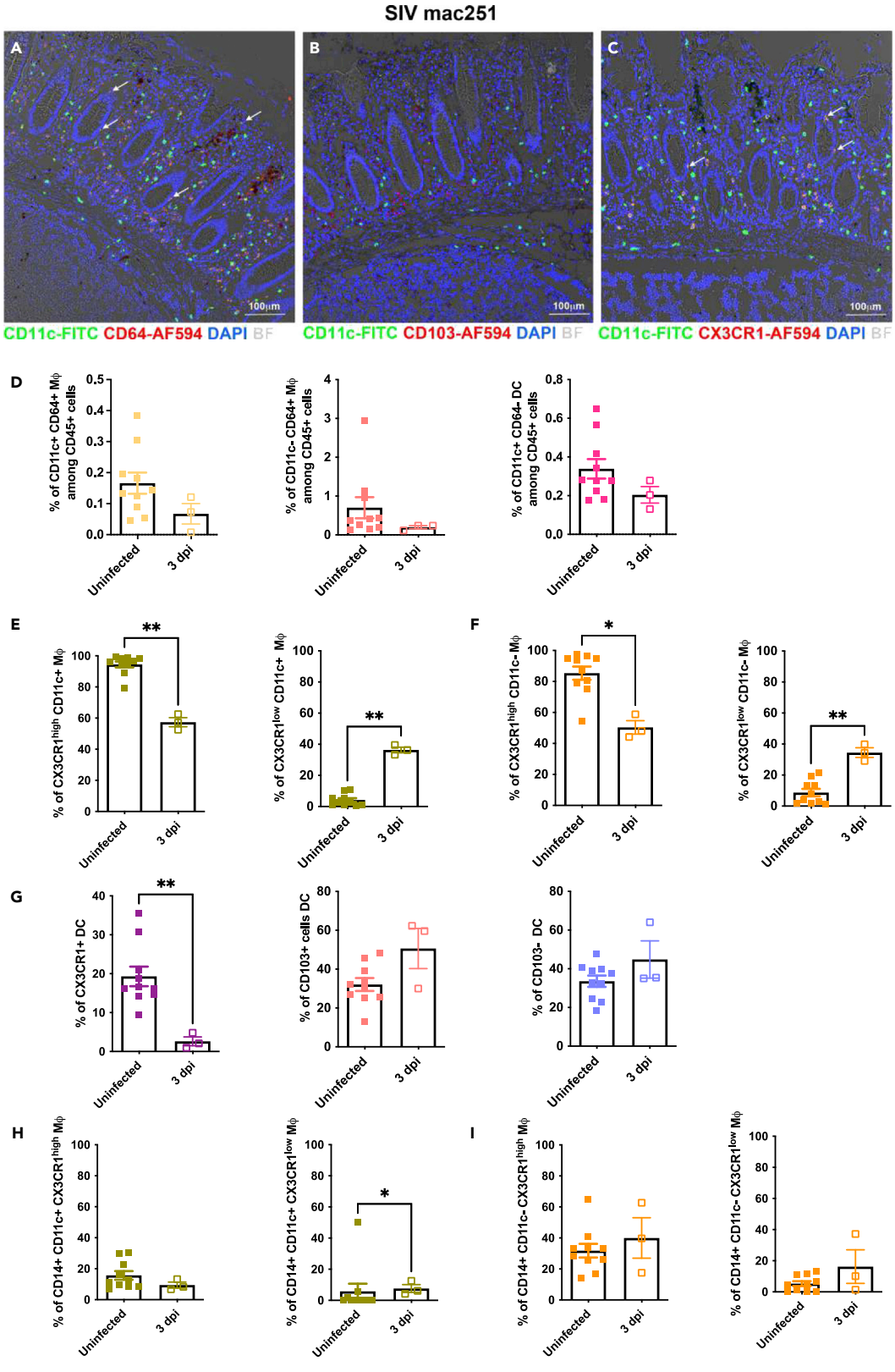
SIV mac251
A
B
C
100μm
CD11c-FITC CD64-AF594 DAPI BF
CD11c-FITC CD103-AF594 DAPI BF
CD11c-FITC CX3CR1-AF594 DAPI BF
D
% of CD11c+ CD64+ Mϕ among CD45+ cells
% of CD11c- CD64+ Mϕ among CD45+ cells
% of CD11c+ CD64- DC among CD45+ cells
E
% of CX3CR1high CD11c+ Mϕ
% of CX3CR1low CD11c+ Mϕ
F
% of CX3CR1high CD11c- Mϕ
% of CX3CR1low CD11c- Mϕ
G
% of CX3CR1+ DC
% of CD103+ cells DC
% of CD103- DC
H
% of CD14+ CD11c+ CX3CR1high Mϕ
% of CD14+ CD11c+ CX3CR1low Mϕ
I
% of CD14+ CD11c- CX3CR1high Mϕ
% of CD14+ CD11c- CX3CR1low Mϕ
Uninfected
3 dpi

Figure 7. Dynamics of colonic mononuclear phagocyte subsets in cynomolgus macaques three days after *in vivo* rectal challenge with SIVmac251

(A–I) Colonic tissues from macaques collected after three days of exposure to SIV, fixed, cryopreserved, and subjected either to immunolabeling for confocal microscopy (A–C) or to collagenase digestion for immune-cell phenotyping by flow cytometry (D–I) are presented. (A–C) Labeling by anti-CD11c-FITC (green) in combination with either CD64 (A), CD103 (B) antibodies followed by goat-*anti*-mouse Alexa Fluor 594 (red), or CX3CR1-PE (C) was performed. Arrows point to subsets of $CD11c^+$ $CD64^+$ (A) and $CD11c^+$ $CX3CR1^+$ (C) cells that migrate from the *lamina propria* to in between the epithelial cells following viral exposure. DAPI (blue) was used to stain the nuclei. The bright field image (BF, gray) was superimposed with the fluorescence images. Scale bars indicate the magnification. (D) Comparable percentages of $CD11c^+$ $CD64^+$ Mφs, $CD11c^-$ $CD6^{4+}$ Mφs, and $CD11c^+$ $CD64^-$ DCs within the total number of $CD45^+$ cells between SIV exposed (n = 3, open symbols) and not exposed (n = 10, filled symbols) macaques are shown. The relative proportion of $CX3CR1^{high}$ and $CX3CR1^{low}$ cells within the $CD11c^+$ $CD64^+$ Mφs (E) and $CD11c^-$ $CD64^+$ Mφs (F); $CX3CR1^+$, $CD103^+$, and $CD103^-$ within $CD11c^+$ $CD64^-$ DCs (G); $CD14^+$ cells within $CD11c^+$ $CX3CR1^{high}$ and CD11c + $CX3CR1^{low}$ (H); and $CD11c^-$ $CX3CR1^{high}$ and $CD11c^-$ $CX3CR1^{low}$ (I) cell populations are plotted. The mean ± the SD is plotted. The Mann-Whitney test was used. p-values < 0.05 were considered significant (*p < 0.05, **p < 0.01, ***p < 0.001).

pathological conditions (Hine and Loke, 2019). Conflicting results have been reported concerning CD14 expression by intestinal Mφs, which may possibly reflect varying conditions under which tissues were obtained. A number of studies described colonic Mφs being mostly $CD14^-$ cells (Caër and Wick, 2020; P. Smith et al., 1997a, 1997b; Smythies et al., 2005), whereas other groups detected an abundant population of $CD14^+$ Mφs (Bernardo et al., 2016, 2018; Bujko et al., 2018), which include tissue resident autofluorescent Mφs (Doyle et al., 2021; Haniffa et al., 2009). Here we show that $CD14^-$ Mφs outnumbered the $CD14^+$ ones in the macaque colonic mucosa at steady-state. An accumulation of pro-inflammatory $CD14^+$ cells has been reported in the colon of AIDS patients (Cassol et al., 2015), and the inflammatory Mφs in HIV-1 infection have been shown to be associated with increased inflammation and tissue damage (Porcheray et al., 2006). Extending these observations, here, we show that CD14 expression specifically increases in $CD11c^+$ $CX3CR1^{low}$ cells in the earliest phase of SIV infection, likely identifying cells of recent gut recruitment. Further studies, possibly including gene expression profiling of FACS-sorted $CX3CR1^{high}$ and $CX3CR1^{low}$ cells, are needed to unravel their functional properties in the context of HIV-1 mucosal infection and to provide useful information for therapeutic intervention for mucosal HIV-1 transmission. Previous studies in humans have indicated that intestinal damage and inflammatory changes begin soon after initial HIV-1 exposure (Appay and Sauce, 2008; Hunt et al., 2014). In nonhuman primate models, the epithelial damage occurs 3 to 14 days post-SIV infection but prior to widespread immune dysfunction (e.g. Th17 depletion) (Hensley-McBain et al., 2018). The loss of $CX3CR1^{high}$ MNPs in our model was observed three days post-SIV exposure and before $CD4^+$ T cell depletion from the colonic *lamina propria*. Given that CX3CR1 is a gatekeeper for intestinal barrier integrity (Medina-Contreras et al., 2011; Schneider et al., 2015), our results highlight $CX3CR1^+$ MNPs as new key players in the pathogenesis of acute HIV-1 infection, possibly contributing to breakdown of the intestinal barrier. Delineating the role of MNP subsets during viral transmission will lead to the fine-tuned characterization of host-virus interactions during the earliest events of colorectal HIV-1 transmission, important for the design of therapeutic approaches. Moreover, it will be of interest to investigate whether the intestinal accumulation of $CX3CR1^{low}$ Mφs increases during chronic HIV infection and whether antiretroviral therapy can restore the $CX3CR1^{high}$ phenotype, similarly to therapies resolving intestinal inflammation.

Limitations of the study

This study has some inherent limitations related to the human and macaque populations. Specifically, the human tissues were obtained from patients undergoing colonic ablation because of cancer, and although the fragments used were morphologically preserved, we cannot fully exclude the persistence of residual inflammation, which could explain the higher abundance of immature $CD11c^+$ Mφs in the human mucosa samples than in nonhuman primates.

We have also provided a proof of concept showing that as soon as three days after *in vivo* viral exposure, the population of colonic $CX3CR1^{high}$ Mφs is partially replaced by cells expressing low levels of the receptor. Further studies in larger cohorts are warranted to confirm the observed phenotypic shift. In addition, the investigation of the functional profile of $CX3CR1^{high}$ versus $CX3CR1^{low}$ Mφs in homeostatic and infection conditions, while overcoming the purposes of the present study, represents an envisaged future development.

STAR★METHODS

Detailed methods are provided in the online version of this paper and include the following:

- KEY RESOURCES TABLE

SUPPLEMENTAL INFORMATION

Supplemental information can be found online at https://doi.org/10.1016/j.isci.2022.104346.

ACKNOWLEDGMENTS

We are grateful for the excellent contributions from the veterinarians and the staff at the IDMIT center. We thank B. Delache and S. Langlois for the handling of the animals, L. Bossevot and M. Leonec for the RT-qPCR experiments, M. Barendji and J. Dinh for the management of NHP biological resources, A. Cosma for assistance with the flow cytometry, and all members of the FlowCyTech, Animal Science and Welfare, L2I, and L3I core facilities. At IRCCS Ospedale San Raffaele microscopy and flow cytometry acquisitions were performed at ALEMBIC and FRACTAL facilities. We thank Dr. Saverio Di Palo (IRCCS Ospedale San Raffaele) for his contribution in the start of the project providing human tissues.

This work was funded by the French Agence Nationale de Recherches sur le Sida et les Hépatites Virales (ANRS, decision n°14415/15516, recipients MC and GS). MC was a beneficiary of a Marie Curie Individual fellowship (grant agreement n° 658277 for the project DCmucoHIV). SD salary was covered by EAVI2020 project funded by the European Union's Horizon 2020 research and innovation program under grant agreement n° 681137.

This work was also supported by the "Programme Investissements d'Avenir" (PIA) managed by the ANR under reference ANR-11-INBS-0008, funding the Infectious Disease Models and Innovative Therapies (IDMIT, Fontenay-aux-Roses, France) infrastructure, and ANR-10-EQPX-02-01, funding the FlowCyTech facility (IDMIT, Fontenay-aux-Roses, France). The funders had no role in the design of the study, data collection or interpretation, or the decision to submit the work for publication.

AUTHOR CONTRIBUTIONS

Study conception and design: MC, GS, and RLG. Acquisition of the data: MC, CF, TS, AF, SD, DD, and NDB. Analysis and interpretation of the data: MC, CF, NDB, and GS. Patients and tissue collection: UE. Draft of the manuscript: MC. Critical revisions: MC, CF, GS and RLG. Funding acquisition: MC, GS, and RLG. All authors read and approved the final version of the manuscript.

DECLARATION OF INTERESTS

The authors declare no competing interests.

Received: December 22, 2021
Revised: March 17, 2022
Accepted: April 28, 2022
Published: June 17, 2022

REFERENCES

Appay, V., and Sauce, D. (2008). Immune activation and inflammation in HIV-1 infection: causes and consequences. J. Pathol. *214*, 231–241. https://doi.org/10.1002/PATH.2276.

Bain, C.C., Bravo-Blas, A., Scott, C.L., Gomez Perdiguero, E., Geissmann, F., Henri, S., Malissen, B., Osborne, L.C., Artis, D., and Mowat, A.M.I. (2014). Constant replenishment from circulating monocytes maintains the macrophage pool in the intestine of adult mice. Nat. Immunol. *15*, 929–937. https://doi.org/10.1038/ni.2967.

Bain, C.C., and Mowat, A.M. (2011). Intestinal macrophages – specialised adaptation to a unique environment. Eur. J. Immunol. *41*, 2494–2498. https://doi.org/10.1002/EJI.201141714.

Bain, C.C., Scott, C.L., Uronen-Hansson, H., Gudjonsson, S., Jansson, O., Grip, O., Guilliams, M., Malissen, B., Agace, W.W., and Mowat, A.M. (2012). Resident and pro-inflammatory macrophages in the colon represent alternative context-dependent fates of the same Ly6Chi monocyte precursors. Mucosal Immunol. *6*, 498–510. https://doi.org/10.1038/mi.2012.89.

Baldwin, J.I., and Baldwin, J.D. (2000). Heterosexual anal intercourse: an understudied, high-risk sexual behavior. Arch. Sex. Behav. *29*, 357–373. https://doi.org/10.1023/A:1001918504344.

Bernardo, D., Durant, L., Mann, E.R., Bassity, E., Montalvillo, E., Man, R., Vora, R., Reddi, D., Bayiroglu, F., Fernández-Salazar, L., et al. (2016). Chemokine (C-C motif) receptor 2 mediates dendritic cell recruitment to the human colon but is not responsible for differences observed in dendritic cell subsets, phenotype, and function between the proximal and distal colon. CMGH *2*, 22–39.e5. https://doi.org/10.1016/j.jcmgh.2015.08.006.

Bernardo, D., Marin, A.C., Fernández-Tomé, S., Montalban-Arques, A., Carrasco, A., Tristán, E., Ortega-Moreno, L., Mora-Gutiérrez, I., Díaz-Guerra, A., Caminero-Fernández, R., et al. (2018). Human intestinal pro-inflammatory CD11chighCCR2+CX3CR1+ macrophages, but not their tolerogenic CD11c−CCR2−CX3CR1− counterparts, are expanded in inflammatory bowel disease. Mucosal Immunol. *11*, 1114–1126. https://doi.org/10.1038/s41385-018-0030-7.

Bradford, B.M., Sester, D.P., Hume, D.A., and Mabbott, N.A. (2011). Defining the anatomical localisation of subsets of the murine mononuclear phagocyte system using integrin alpha X (Itgax, CD11c) and colony stimulating factor 1 receptor (Csf1r, CD115) expression fails to discriminate dendritic cells from macrophages. Immunobiology *216*, 1228–1237. https://doi.org/10.1016/j.imbio.2011.08.006.

Bujko, A., Atlasy, N., Landsverk, O.J.B., Richter, L., Yaqub, S., Horneland, R., Øyen, O., Aandahl, E.M., Aabakken, L., Stunnenberg, H.G., et al. (2018). Transcriptional and functional profiling defines human small intestinal macrophage subsets. J. Exp. Med. *215*, 441–458. https://doi.org/10.1084/jem.20170057.

Caër, C., and Wick, M.J. (2020). Human intestinal mononuclear phagocytes in Health and inflammatory bowel disease. Front. Immunol. *11*, 410. https://doi.org/10.3389/FIMMU.2020.00410.

Cassol, E.T., Rossouw, S., Malfeld, P., Mahasha, T., Slavik, C., Seebregts, R., Bond, J., du Plessis, C., Janssen, T., Roskams, F., et al. (2015). CD14(+) macrophages that accumulate in the colon of African AIDS patients express pro-inflammatory cytokines and are responsive to lipopolysaccharide. BMC Infect. Dis. *15*, 430. https://doi.org/10.1186/S12879-015-1176-5.

Cavarelli, M., Foglieni, C., Rescigno, M., and Scarlatti, G. (2013). R5 HIV-1 envelope attracts dendritic cells to cross the human intestinal epithelium and sample luminal virions via engagement of the CCR5. EMBO Mol. Med. *5*, 776–794. https://doi.org/10.1002/emmm.201202232.

Cavarelli, M., Hua, S., Hantour, N., Tricot, S., Tchitchek, N., Gommet, C., Hocini, H., Chapon, C., Dereuddre-Bosquet, N., and Le Grand, R. (2021). Leukocytospermia induces intraepithelial recruitment of dendritic cells and increases SIV replication in colorectal tissue explants. Commun. Biol. *4*, 861. https://doi.org/10.1038/S42003-021-02383-9.

Cavarelli, M., and Scarlatti, G. (2014). HIV-1 infection: the role of the gastrointestinal tract. Am. J. Reprod. Immunol. *71*, 537–542. https://doi.org/10.1111/aji.12245.

Cerovic, V., Bain, C.C., Mowat, A.M., and Milling, S.W.F. (2014). Intestinal macrophages and dendritic cells: what's the difference? Trends Immunol. *35*, 270–277. https://doi.org/10.1016/J.IT.2014.04.003.

Chiaranunt, P., Tai, S.L., Ngai, L., and Mortha, A. (2021). Beyond immunity: underappreciated functions of intestinal macrophages. Front. Immunol. *12*, 3866. https://doi.org/10.3389/FIMMU.2021.749708.

Coleman, C.M., and Wu, L. (2009). HIV interactions with monocytes and dendritic cells: viral latency and reservoirs. Retrovirology *6*, 51. https://doi.org/10.1186/1742-4690-6-51.

Desalegn, G., and Pabst, O. (2019). Inflammation triggers immediate rather than progressive changes in monocyte differentiation in the small intestine. Nat. Commun. *10*, 3229–3314. https://doi.org/10.1038/s41467-019-11148-2.

Doyle, C.M., Vine, E.E., Bertram, K.M., Baharlou, H., Rhodes, J.W., Dervish, S., Gosselink, M.P., Di Re, A., Collins, G.P., Reza, F., et al. (2021). Optimal isolation protocols for examining and interrogating mononuclear phagocytes from human intestinal tissue. Front. Immunol. *12*, 3481. https://doi.org/10.3389/FIMMU.2021.727952.

Ganor, Y., Real, F., Sennepin, A., Dutertre, C.A., Prevedel, L., Xu, L., Tudor, D., Charmeteau, B., Couedel-Courteille, A., Marion, S., et al. (2019). HIV-1 reservoirs in urethral macrophages of patients under suppressive antiretroviral therapy. Nat. Microbiol. *4*, 633–644. https://doi.org/10.1038/s41564-018-0335-z.

Grainger, J.R., Konkel, J.E., Zangerle-Murray, T., and Shaw, T.N. (2017). Macrophages in gastrointestinal homeostasis and inflammation. Pflugers Arch. *469*, 527–539. https://doi.org/10.1007/S00424-017-1958-2.

Han, X., Ding, S., Jiang, H., and Liu, G. (2021). Roles of macrophages in the development and treatment of gut inflammation. Front. Cell Dev. Biol. *9*, 625423. https://doi.org/10.3389/FCELL.2021.625423/BIBTEX.

Haniffa, M., Ginhoux, F., Wang, X.N., Bigley, V., Abel, M., Dimmick, I., Bullock, S., Grisotto, M., Booth, T., Taub, P., et al. (2009). Differential rates of replacement of human dermal dendritic cells and macrophages during hematopoietic stem cell transplantation. J. Exp. Med. *206*, 371–385. https://doi.org/10.1084/JEM.20081633.

Hensley-McBain, T., Berard, A.R., Manuzak, J.A., Miller, C.J., Zevin, A.S., Polacino, P., Gile, J., Agricola, B., Cameron, M., Hu, S.-L.L., et al. (2018). Intestinal damage precedes mucosal immune dysfunction in SIV infection. Mucosal Immunol. *11*, 1429–1440. https://doi.org/10.1038/s41385-018-0032-5.

Hine, A.M., and Loke, P. (2019). Intestinal macrophages in resolving inflammation. J. Immunol. *203*, 593–599. https://doi.org/10.4049/JIMMUNOL.1900345.

Ho, D.D., Rota, T.R., and Hirsch, M.S. (1986). Infection of monocyte/macrophages by human T lymphotropic virus type III. J. Clin. Invest. *77*, 1712–1715. https://doi.org/10.1172/JCI112491.

Hunt, P.W., Sinclair, E., Rodriguez, B., Shive, C., Clagett, B., Funderburg, N., Robinson, J., Huang, Y., Epling, L., Martin, J.N., et al. (2014). Gut epithelial barrier dysfunction and innate immune activation predict mortality in treated HIV infection. J. Infect. Dis. *210*, 1228–1238. https://doi.org/10.1093/INFDIS/JIU238.

Joeris, T., Müller-Luda, K., Agace, W.W., and Mowat, A.M. (2017). Diversity and functions of intestinal mononuclear phagocytes. Mucosal Immunol. *10*, 845–864. https://doi.org/10.1038/mi.2017.22.

Kayama, H., Ueda, Y., Sawa, Y., Jeon, S.G., Ma, J.S., Okumura, R., Kubo, A., Ishii, M., Okazaki, T., Murakami, M., et al. (2012). Intestinal CX3C chemokine receptor 1high (CX3CR1high) myeloid cells prevent T-cell-dependent colitis. Proc. Natl. Acad. Sci. U S A *109*, 5010–5015. https://doi.org/10.1073/PNAS.1114931109.

Kumar, A., Abbas, W., and Herbein, G. (2014). HIV-1 latency in monocytes/macrophages. Viruses *6*, 1837–1860. https://doi.org/10.3390/V6041837.

Li, J., Zhou, H., Fu, X., Zhang, M., Sun, F., and Fan, H. (2021). Dynamic role of macrophage CX3CR1 expression in inflammatory bowel disease. Immunol. Lett. *232*, 39–44. https://doi.org/10.1016/J.IMLET.2021.02.001.

Li, L., Meng, G., Graham, M.F., Shaw, G.M., and Smith, P.D. (1999). Intestinal macrophages display reduced permissiveness to human immunodeficiency virus 1 and decreased surface CCR5. Gastroenterology *116*, 1043–1053. https://doi.org/10.1016/S0016-5085(99)70007-7.

McElrath, M.J., Smythe, K., Randolph-Habecker, J., Melton, K.R., Goodpaster, T.A., Hughes, S.M., MacK, M., Sato, A., Diaz, G., Steinbach, G., et al. (2013). Comprehensive assessment of HIV target cells in the distal human gut suggests increasing

HIV susceptibility toward the anus. J. Acquir. Immune Defic. Syndr. *63*, 263–271. https://doi.org/10.1097/QAI.0b013e3182898392.

Medina-Contreras, O., Geem, D., Laur, O., Williams, I.R., Lira, S.A., Nusrat, A., Parkos, C.A., and Denning, T.L. (2011). CX3CR1 regulates intestinal macrophage homeostasis, bacterial translocation, and colitogenic Th17 responses in mice. J. Clin. Invest. *121*, 4787–4795. https://doi.org/10.1172/JCI59150.

Misegades, L., Page-Shafer, K., Halperin, D., and McFarland, W. (2001). Anal intercourse among young low-income women in California: an overlooked risk factor for HIV? AIDS *15*, 534–535. https://doi.org/10.1097/00002030-200103090-00017.

Moore, A.C., Bixler, S.L., Lewis, M.G., Verthelyi, D., and Mattapallil, J.J. (2012). Mucosal and peripheral Lin- HLA-DR+ CD11c/123- CD13+ CD14- mononuclear cells are preferentially infected during acute simian immunodeficiency virus infection. J. Virol. *86*, 1069–1078. https://doi.org/10.1128/JVI.06372-11.

Mowat, A.M., and Agace, W.W. (2014). Regional specialization within the intestinal immune system. Nat. Rev. Immunol. *14*, 667–685. https://doi.org/10.1038/nri3738.

Lee, M., Lee, Y., Song, J., Lee, J., and Chang, S.-Y. (2018). Tissue-specific role of CX3CR1 expressing immune cells and their Relationships with human disease. Immune Netw. *18*, e5. https://doi.org/10.4110/IN.2018.18.E5.

Niess, J.H., Brand, S., Gu, X., Landsman, L., Jung, S., McCormick, B.A., Vyas, J.M., Boes, M., Ploegh, H.L., Fox, J.G., et al. (2005). CX3CR1-mediated dendritic cell access to the intestinal lumen and bacterial clearance. Science *307*, 254–258. https://doi.org/10.1126/science.1102901.

Persson, E.K., Scott, C.L., Mowat, A.M., and Agace, W.W. (2013). Dendritic cell subsets in the intestinal lamina propria: ontogeny and function. Eur. J. Immunol. *43*, 3098–3107. https://doi.org/10.1002/EJI.201343740.

Porcheray, F., Samah, B., Léone, C., Dereuddre-Bosquet, N., and Gras, G. (2006). Macrophage activation and human immunodeficiency virus infection: HIV replication directs macrophages towards a pro-inflammatory phenotype while previous activation modulates macrophage susceptibility to infection and viral production. Virology *349*, 112–120. https://doi.org/10.1016/J.VIROL.2006.02.031.

Rhodes, J.W., Botting, R.A., Bertram, K.M., Vine, E.E., Rana, H., Baharlou, H., Vegh, P., O'Neil, T.R., Ashhurst, A.S., Fletcher, J., et al. (2021). Human anogenital monocyte-derived dendritic cells and langerin+cDC2 are major HIV target cells. Nat. Commun. *12*, 2147–2215. https://doi.org/10.1038/s41467-021-22375-x.

Sagaert, X., Tousseyn, T., and De Hertogh, G. (2012). Macrophage-related diseases of the gut: a pathologist's perspective. Virchows Arch. *460*, 555–567. https://doi.org/10.1007/S00428-012-1244-9.

Schneider, K.M., Bieghs, V., Heymann, F., Hu, W., Dreymueller, D., Liao, L., Frissen, M., Ludwig, A., Gassler, N., Pabst, O., et al. (2015). CX3CR1 is a gatekeeper for intestinal barrier integrity in mice: limiting steatohepatitis by maintaining intestinal homeostasis. Hepatology *62*, 1405–1416. https://doi.org/10.1002/hep.27982.

Schulz, O., Jaensson, E., Persson, E.K., Liu, X., Worbs, T., Agace, W.W., and Pabst, O. (2009). Intestinal CD103+, but not CX3CR1+, antigen sampling cells migrate in lymph and serve classical dendritic cell functions. J. Exp. Med. *206*, 3101–3114. https://doi.org/10.1084/jem.20091925.

Shen, R., Richter, H.E., Clements, R.H., Novak, L., Huff, K., Bimczok, D., Dandekar, S., Clapham, P.R., Smythies, P.D., and Smith, P.D. (2009). Macrophages in vaginal but not intestinal mucosa are monocyte-like and permissive to human immunodeficiency virus type 1 infection. J. Virol. *83*, 3258–3267. https://doi.org/10.1128/JVI.01796-08.

Shen, R., Smythies, L.E., Clements, R.H., Novak, L., and Smith, P.D. (2010). Dendritic cells transmit HIV-1 through human small intestinal mucosa. J. Leukoc. Biol. *87*, 663–670. https://doi.org/10.1189/jlb.0909605.

Smith, P.D., Janoff, M., Mosteller-Barnum, M., Merger, M., Orenstein, J.M., Kearney, J.F., and Graham, M.F. (1997a). Isolation and purification of CD14-negative mucosal macrophages from normal human small intestine. J. Immunol. Methods *202*, 1–11. https://doi.org/10.1016/S0022-1759(96)00204-9.

Smith, P.D., Meng, G., Shaw, G.M., and Li, L. (1997b). Infection of gastrointestinal tract macrophages by HIV-1. J. Leukoc. Biol. *62*, 72–77. https://doi.org/10.1002/jlb.62.1.72.

Smythies, L.E., Sellers, R.H., Clements, R.H., Clement, M., Mosteller-Barnum, G., Meng, W.H., Benjamin, J.M., Orenstein, P.D., and Smith, P.D. (2005). Human intestinal macrophages display profound inflammatory anergy despite avid phagocytic and bacteriocidal activity. J. Clin. Invest. *115*, 66–75. https://doi.org/10.1172/JCI19229.

Tamoutounour, S., Henri, S., Lelouard, H., de Bovis, B., de Haar, C., van der Woude, C.J., Woltman, A.M., Reyal, Y., Bonnet, D., Sichien, D., et al. (2012). CD64 distinguishes macrophages from dendritic cells in the gut and reveals the Th1-inducing role of mesenteric lymph node macrophages during colitis. Eur. J. Immunol. *42*, 3150–3166. https://doi.org/10.1002/eji.201242847.

Varol, C.A., Vallon-Eberhard, A., Vallon-Eberhard, E., Elinav, E., Elina, T., Aychek, Y., Shapira, H., Luche, H.J., Fehling, W.D., Hardt, G., et al. (2009). Intestinal lamina propria dendritic cell subsets have different origin and functions. Immunity *31*, 502–512. https://doi.org/10.1016/J.IMMUNI.2009.06.025.

Weber, B., Saurer, L., Schenk, M., Dickgreber, N., and Mueller, C. (2011). CX3CR1 defines functionally distinct intestinal mononuclear phagocyte subsets which maintain their respective functions during homeostatic and inflammatory conditions. Eur. J. Immunol. *41*, 773–779. https://doi.org/10.1002/EJI.201040965.

Zalar, A., Figueroa, M.I., Ruibal-Ares, P., Barè, P., Cahn, M.M., de Bracco, M.M.D.E., and Belmonte, L. (2010). Macrophage HIV-1 infection in duodenal tissue of patients on long term HAART. Antivir. Res. *87*, 269–271. https://doi.org/10.1016/J.ANTIVIRAL.2010.05.005.

Zigmond, E., Bernshtein, B., Friedlander, G., Walker, C.R., Walker, C., Yona, S., Kim, K.W., Brenner, O., Krauthgamer, R., Varol, C., et al. (2014). Macrophage-restricted interleukin-10 receptor deficiency, but not IL-10 deficiency, causes severe spontaneous colitis. Immunity *40*, 720–733. https://doi.org/10.1016/J.IMMUNI.2014.03.012.

STAR★METHODS

KEY RESOURCES TABLE

REAGENT or RESOURCE	SOURCE	IDENTIFIER
Antibodies		
CD45-V500	BD	Cat# 560779; RRID: AB_1937332
CD45-PerCp	BD	Cat# 558411; RRID: AB_397080
CD3-PER-CP-Cy5.5	BD	Cat# 560835; RRID: AB_2033956
CD3-V500	BD	Cat# 560770; RRID: AB_1937322
CD8-BV650	BD	Cat# 563821; RRID: AB_2744462
CD14-Alexafluor700	BD	Cat# 557923; RRID: AB_396944
CD16-PER-CP-Cy5.5	BD	Cat# 560717; RRID: AB_1727434
CD16-PE-CF594	BD	Cat# 562293; RRID: AB_11151916
CD19-PER-CP-Cy5.5	BD	Cat# 332780; RRID: AB_2868629
CD20-BV711	BD	Cat# 563126; RRID: AB_2313579
CD56-PER-CP-Cy5.5	BD	Cat# 560842; RRID: AB_2033964
HLA-DR APC	BD	Cat# 559866; RRID: AB_398674
HLA-DR APC-H7	BD	Cat# 561358; RRID: AB_10611876
CD11c-PB	Biolegend	Cat# 301625; RRID: AB_10662901
CD11c-APC	BD	Cat# 333144; RRID: AB_2868645
CD123-PE-Cy7	BD	Cat# 560826; RRID: AB_10563898
CD64-PE-CF594	BD	Cat# 565389; RRID: AB_2739213
CD64-V450	BD	Cat# 561202; RRID: AB_10564066
CD103-PE	ebioscience	Cat# 12-1038; RRID: AB_11150242
CX3CR1-FITC	Biolegend	Cat# 341605; RRID: AB_1626276
CXCR4-PE	BD	Cat# 555974; RRID: AB_396267
CXCR4-PECF594	BD	Cat# 562389; RRID: AB_11153132
CCR5-FITC	BD	Cat# 555992; RRID: AB_396278
CCR5-BV421	BD	Cat# 565000; RRID: AB_2739038
CD3	BD	Cat# 551916; RRID: AB_394293
CD11c-FITC	Invitrogen	Cat# MHCD11c01; RRID: AB_10373970
CD64	BD	Cat# 555525; RRID: AB_395911
CD103	AbDSerotec	Cat# MCA708T; RRID: AB_1100549
CX3CR1-PE	Biolegend	Cat# 355704; RRID: AB_2561681
Bacterial and virus strains		
HIV-1 AD8	Cavarelli et al., 2013 ; https://doi.org/10.1002/emmm.201202232	N/A
SIVmac251 isolate	Cavarelli et al., 2013; https://doi.org/10.1038/s42003-021-02383-9.	N/A
Biological samples		
Human colon samples	IRCCS Ospedale San Raffaele, Milan, Italy	https://www.hsr.it
Macaque colon samples	ICEA, MVA-HB/IDMIT, Fonteney-aux-Roses, France	https://www.idmitcenter.fr

(*Continued on next page*)

Continued

REAGENT or RESOURCE	SOURCE	IDENTIFIER
Critical commercial assays		
Superscript III Platinum one-step quantitative RT-PCR system	Invitrogen	11732088
RETRO-TEK SIV p27 Ag ELISA kit	Helvetica Health Care	0801169
Software and algorithms		
Prism	GraphPad	https://www.graphpad.com
BD FACSDiva	BD	https://www.bdbiosciences.com
FlowJo	BD	https://www.flowjo.com
Image J	NIH	https://imagej.nih.gov/
PhotoshopCS	Adobe	https://www.adobe.com/

RESOURCE AVAILABILITY

Lead contact

Further information and requests for resources and reagents should be directed to and will be fulfilled by the lead contact Mariangela Cavarelli (mariangela.cavarelli@cea.fr).

Materials availability

This study did not generate new unique reagents. The authors declare that all data supporting the findings of this study are available within the article and its supplemental information files or are available from the authors upon request.

Data and code availability

Any additional information required to reanalyze the data reported in this paper is available from the Lead contact upon request.

EXPERIMENTAL MODEL AND SUBJECT DETAILS

Ethical statement and animal care

The study protocol for human mucosal tissues was approved by the institutional Ethics committee of IRCCS Ospedale San Raffaele (MUCHIV protocol Ethical Committee approval #35 06/02/2014 and extension #40 09/11/2015). Patients were followed at the Department of General and Gastrosurgery, IRCCS Ospedale San Raffaele, and signed the informed consent form.

Cynomolgus macaques (*Macaca fascicularis*), originating from Mauritian AAALAC certified breeding centers, were used in this study. All animals were housed in the IDMIT facilities (CEA, Fontenay-aux-Roses) under BSL-3 containment (Animal facility authorization #D92-032-02, Préfecture des Hauts de Seine, France) and in compliance with European Directive 2010/63/EU, French regulations, and the Standards for Human Care and Use of Laboratory Animals. All work related to animals was conducted in compliance with institutional guidelines and protocols approved by the local ethics committee "Comité d'Ethique en Expérimentation Animale du Commissariat à l'Energie Atomique et aux Energies Alternatives" (CEtEA #44). The study was authorized by the "Research, Innovation and Education Ministry" under registration number APAFIS#6058-20 1607121 0017243. Sigmoid colon and draining colon lymph nodes were collected during animal necropsies.

Study design and sample utilization

Human colonic samples were obtained from 20 patients with invasive colon cancer but without HIV-1 infection (55% females, age 63.9 $\pm$ 13.3 years [mean $\pm$ standard deviation], age range 44 to 89 years). Sections of sigmoid or descending (close to the sigmoid) colon from morphologically normal tissue (distal from the site of the pathology) were obtained from leftover surgical tissue of intestinal resections. Among them, 17 samples were used to carry out immune-cell phenotyping (panel for lamina propria mononuclear cells,

summarized in Table S1) and three for *ex vivo* virus exposure experiments and confocal microscopy analysis.

Twenty-one cynomolgus macaques (67% females, age 4.7 ± 1 years [mean ± standard deviation], weight range 3.8 to 7.5 kg), including 18 uninfected controls and three animals exposed to SIVmac251 *in vivo* and sacrificed three days later, were used. All animals were negative for antibody responses to SIV, simian retrovirus type D (SRV), and simian T-cell lymphotropic virus (STLV) at the beginning of the study. Eighteen colon samples (n = 15 SIV- and n = 3 SIV-exposed) and six lymph nodes draining the colon (LN, n = 3 SIV- and n = 3 SIV-exposed) were used to carry out immune-cell phenotyping (Table S1). Colon tissue from 3 SIV^- donors was used for *ex vivo* virus exposure experiments and confocal microscopy analysis.

METHOD DETAILS

Virus production

HIV-1 AD8 infectious molecular clone was produced by transfection of 293T cells with the pAD8 plasmid using Fugene 6 (Roche, Indianapolis, IN, USA), as previously described (Cavarelli et al., 2013). The SIVmac251 viral isolate used for the *in vivo* experiments was kindly provided by Dr A.M. Aubertin (Université Louis Pasteur, Strasbourg, France). The titer, determined after intra-rectal inoculation, was 100 AID50/mL. For *ex vivo* explant experiments, the SIVmac251 isolate was expanded in CEMx174 cells grown in RPMI medium. Cells (30×10^6) were incubated at a multiplicity of infection (MOI) of 10^{-2} for 2 h at 37°C and the volume adjusted to 1×10^6 cells/mL. Cultures were maintained for 21 days, changing half of the cells every 3 to 4 days. Viral replication was monitored by measuring p27 levels in culture supernatants by ELISA (RETRO-TEK SIV p27 Ag ELISA kit, Helvetica Health Care). Cell-free viral stock was passed through a 0.2-μm pore-size filter, aliquoted, and stored at −80°C.

Isolation and phenotyping of lamina propria mononuclear and lymph-node cells

Macaque draining colon lymph-node cells were obtained by mechanical dissociation. To isolate lamina propria mononuclear cells (LPMCs), both human and macaque sigmoid colons were cut into small pieces and incubated for 20 min at 37°C in HBSS medium without Ca^{++}/Mg^{++} (Fisher Scientific, Illkirch, France) supplemented with 5 mM EDTA and 1 mM DTT (Sigma-Aldrich, St Quantin Fallavier, France) to eliminate mucus and epithelial cells. After washing in PBS, the tissue was incubated for 1 h at 37°C with agitation in HBSS medium with Ca^{++}/Mg^{++} (Fisher Scientific, Illkirch, France) containing collagenase type VIII (0.25 mg/mL, Sigma Aldrich, St Quantin Fallavier, France) and DNase (5 U/mL, Roche, Mannheim, Germany). Undigested pieces were submitted to a second digestion for 30 min. Cell suspensions from lymph nodes or colon were filtered through 70-mm sterile nylon cell strainers (BD Biosciences), washed with complete medium (RPMI supplemented with 10% FCS, 100 U/mL penicillin/streptomycin, 1% glutamine, 1% NEAA, 1% Na-pyruvate, 1% HEPES buffer [1 M]; all from Fisher Scientific, Illkirch, France) and analyzed by flow cytometry. Antibodies used for the staining of human and macaque cells are listed in Table S2. Human cell phenotypes were acquired on a Navios Ex flow cytometer (Beckman Coulters) at Ospedale San Raffaele, and macaque cell phenotypes on an LSR Fortessa (BD Biosciences) at the IDMIT institute. All results were analyzed using FlowJo 9.8.3 (Tristar, USA) software within the singlet viable fraction. Positive and negative gating was set using the fluorescence minus one (FMO) method.

Polarized *ex vivo* explant culture

Human colonic fragments and macaque sigmoid colon were collected in cold PBS supplemented with 100 U/mL penicillin/streptomycin and 50 mg/mL gentamicin and then processed for *ex vivo* culture within 30 to 45 min from excision, as previously described (Cavarelli et al., 2013, 2021). Briefly, after abundant washing in the same solution, the specimens were transferred into complete medium and the epithelial surface exposed. For polarized *ex vivo* culture, tissue explants (diameter 8.0 mm), including the epithelium and sub-mucosa, were cut out with a biopsy punch (Stiefel, Laboratories, Inc. North Carolina) and placed on a sponge support (area = 2.25 cm^2, BioOptica, Milan, Italy) with the sub-mucosa facing the sponge. A polystyrene cylinder (I.D. x H 4.7 × 8 mm, Sigma-Aldrich, St. Louis, MO) was sealed with veterinary glue (3M Vetbond, St. Paul, MN) onto the apical surface of the mucosa to avoid leakage. Specimens were placed in a 60-mm center-well organ culture dish (BD Falcon, San Diego, CA) containing 1 mL complete medium.

Mucosal explant cultures were treated apically with 100 μL viral culture supernatant (HIV-1 AD8, SIVmac251) or complete medium as a negative control. After 30 min, the apical stimulus was halted, the tissues washed

six times with PBS, and then fixed in 4% paraformaldehyde (PFA) for 4 hours at 4°C, cryoprotected in 10% sucrose over-night at 4°C, embedded in optimal cutting temperature embedding medium (OCT compound, VWR, Milan, Italy), and snap-frozen. One explant was fixed before the establishment of the tissue culture to serve as a time zero control.

Histopathology analysis, immunofluorescence markers, and confocal microscopy

Tissue preservation was verified under a light microscope (Nikon Eclipse 80i) for all tissues on at least three 5-μm thick cryosections taken 100 μm apart and stained with Hematoxylin/Eosin. For confocal microscopy analysis of colonic tissues, at least 5 to 6 serially cut 10-μm thick sections, sampled 100 μm apart, were obtained. The antibodies used for confocal microscopy phenotyping are listed in Table S3. Primary antibodies were used at a final concentration of 10 μg/mL and were omitted from the methodological negative control sections. Single-channel images from Z-series were collected from at least three representative fields/labelling/sample using a Leica TCS SP8 confocal microscope (Leica Microsystems GmbH, Wetzlar Germany) and the images processed using Image J 1.49v and PhotoshopCS software. Human and macaque tissues were independently processed at the IRCCS Ospedale San Raffaele and at the IDMIT center, respectively.

In vivo infection, sample collection, and quantification of blood viral load of cynomolgus macaques

Three adults male cynomolgus macaques were intrarectally exposed to 50 animal infectious doses 50 (50 AID50) of SIVmac251 isolate and sacrificed three days later by intravenous injection of 180 mg/kg sodium pentobarbital. Blood samples were collected twice in BD VacutainerR Plus Plastic K3EDTA tubes for plasma viral load quantification, i.e., before viral exposure from sedated animals following 5 mg/kg intra-muscular injection of ZoletilR 100 (Virbac, Carros, France) and at necropsy. The sigmoid colon and draining colon lymph nodes were collected at necropsy. Punches of the colonic tissue (6 mm in diameter, n = 2/donor) were immediately fixed in 4% PFA, processed as above, and snap-frozen. The remaining tissue was subjected to collagenase digestion, as described above.

Plasma was isolated from EDTA blood by centrifugation for 10 min at 1,500 × g and cryopreserved at −80°C. Blood viral RNA was obtained from 250 μL cell-free plasma using the Nucleospin 96 RNA kit (Macherey Nagel GmbH&Co KG, Düren, Germany), according to the manufacturer's instructions. Retrotranscription and cDNA amplification and quantification were performed in duplicate by RT-qPCR using the Superscript III Platinum one-step quantitative RT-PCR system (Invitrogen, Carlsbad, USA). RT-PCR was performed as previously described (Cavarelli et al., 2021). The quantification limit (QL) was estimated to be 111 copies/mL and the detection limit (DL) 37 copies/mL.

QUANTIFICATION AND STATISTICAL ANALYSIS

All data visualization and statistical analyses were carried out using Prism v9.2.0 software (GraphPad software, La Jolla, USA). The statistical significance of differences between two groups was tested using Mann-Whitney U tests or Wilcoxon signed rank tests. The statistical significance of differences between more than two groups was tested using Friedman tests and p values were corrected for multiple comparisons using the Benjamini, Krieger, and Yekutieli FDR approach. p values ≤ 0.05 for two-tailed tests were considered significant, *$p < 0.05$, **$p < 0.01$, ***$p < 0.001$, ****$p < 0.0001$.